Journal of Controlled Release 358 (2023) 420–438

Contents lists available at ScienceDirect

Journal of Controlled Release

journal homepage: www.elsevier.com/locate/jconrel

# Efficient colonic drug delivery in domestic pigs employing a tablet formulation with dual control concept

Viviane Doggwiler [a,b], Chasper Puorger [a], Valeria Paredes [a], Michael Lanz [a], Katja M. Nuss [c], Georg Lipps [a], Georgios Imanidis [a,b,*]

[a] School of Life Sciences, University of Applied Sciences Northwestern Switzerland, Hofackerstrasse 30, 4132 Muttenz, Switzerland
[b] Department of Pharmaceutical Sciences, University of Basel, Klingelbergstrasse 50, 4056 Basel, Switzerland
[c] Musculoskeletal Research Unit, Vetsuisse Faculty, University of Zurich, Winterthurerstrasse 204, 8057 Zurich, Switzerland

ARTICLE INFO

*Keywords:*
Colonic drug delivery
Physiologically based pharmacokinetic modeling
Pharmacokinetic deconvolution
Domestic pig
Telemetric capsule

ABSTRACT

Efficient and reproducible colonic drug delivery remains elusive. The aim of this study was to demonstrate specific colonic delivery *in vivo* in domestic pigs with a novel tablet formulation based on a dual release control concept using 5-aminosalicylic acid (5-ASA) and caffeine as drug substances. The developed controlled colonic release (CCR) tablet formulation employs a pH-sensitive coating based on Eudragit® FS 30 D to prevent drug release in the upper gastrointestinal tract, and a xyloglucan-based matrix to inhibit drug release after coating removal in the small intestine and to allow microbiome-triggered drug release by enzymatic action in the colon. CCR tablets were administered to domestic pigs and plasma concentration data was analyzed by physiologically based pharmacokinetic modeling to estimate absorbed amounts from small and large intestine and *in vivo* drug release rates by model-dependent deconvolution using immediate release (IR) tablets and intravenous solutions as reference. Peak concentration times ($t_{max}$) and values ($c_{max}$) of CCR 5-ASA and caffeine tablets indicated strongly delayed drug absorption and the deduced absorbed amount as a function of time confirmed absorption overwhelmingly from the large intestine. The microbially cleaved marker molecule sulfasalazine administered alone or together with caffeine in CCR tablets reported, in combination with telemetry measurements, gastrointestinal transit times and site of absorption. Drug release from CCR tablets was inferred to take place predominantly at the site of absorption at a release rate of caffeine that was much larger in the colon than in the small intestine indicating enzymatically triggered release by the colonic microbiome. Xyloglucanase activity in rectal and cecal samples was consistent with release data and compound recovery in fecal droppings was consistent with 5-ASA bioavailability. The results provide evidence that the developed formulation can prevent premature drug release and provide targeted colonic drug delivery. Clinical relevance based on the comparability between pig and man is discussed.

## 1. Introduction

Drug delivery to the colon is currently exploited for the local treatment of inflammatory bowel diseases (IBD). The topically active anti-inflammatory agent 5-aminosalicylic acid (5-ASA) is administered as first-line therapy for the treatment of mild-to-moderate disease forms [1]. Oral formulations aiming to target the large intestine must prevent both premature drug release in the upper gastrointestinal tract and drug loss in the feces. Strategies reported in the literature for colonic delivery are based on differences between gastrointestinal segments with respect to transit time, pH, or bacterial count [2]. Commercial peroral 5-ASA formulations predominantly rely on pH sensitive coating layers intended to dissolve during transit through the lower small intestine. Inherent variability of pH values along the entire gastrointestinal tract, however,

*Abbreviations:* 4-ASA, 4-aminosalicylic acid; 5-ASA, 5-aminosalicylic acid; Ac-5-ASA, N-Acetyl-5-aminosalicylic acid; API, active pharmaceutical ingredient; AUC, area under the curve; BW, body weight; CAT, colonic arrival time; CCR, controlled colonic release; CTT, colonic transit time; GET, gastric emptying time; IBD, inflammatory bowel disease; im, intramuscular; IR, immediate release; iv, intravenous; PBPK, physiologically based pharmacokinetic modeling; PBS, phosphate buffered saline; SITT, small intestinal transit time; WGTT, whole gut transit time.

* Corresponding author at: School of Life Sciences, University of Applied Sciences Northwestern Switzerland, Hofackerstrasse 30, 4132 Muttenz, Switzerland.
*E-mail address:* georgios.imanidis@unibas.ch (G. Imanidis).

https://doi.org/10.1016/j.jconrel.2023.04.047
Received 23 February 2023; Received in revised form 20 April 2023; Accepted 27 April 2023
Available online 13 May 2023

reportedly cause premature coating dissolution in the stomach and upper small intestine, or insufficient coating removal and subsequent defecation of tablets [3–5]. In both cases formulations fail to deliver drugs to the targeted site. The use of a composite coating that is responsive to pH changes and bacterial enzyme action party in combination with multiple coating layers has been in the focus of recent research for improved colonic delivery by achieving fail-safe coating dissolution in the colon [6–8] and demonstrated accurate drug release at the target site using a rather complex triple tablet coating [9]. Of the other approaches, delayed-release formulations relying on the rather constant small intestinal transit time of 3 ± 1 h [10] persistently showed a variable onset of drug release even after the addition of an enteric coating to alleviate variable gastric retention [8,11]. The enzymatic trigger of the colonic microbiome is utilized by the commercially available prodrug sulfasalazine for colonic release of 5-ASA [12] and has been investigated in connection with bacterially degradable polysaccharides as matrix formers and coatings, whereby the employed materials failed to combine a satisfactory retardation of drug release in the upper gastrointestinal tract with a sufficient response to microbial degradation [13–15]. A comprehensive review of the employed approaches for accomplishing colonic delivery was recently given [16].

The present authors have developed and characterized *in vitro* a combination of an enteric coating with a non-readily disintegrating but bacterially degradable polysaccharide matrix in a tablet formulation for controlled colonic release (CCR) [16]. These CCR tablets utilize two physiologically triggered release controlling mechanisms for efficient and selective colonic drug delivery. *In vitro* tests showed that the pH sensitive Eudragit® FS coating layer prevented drug release in upper gastrointestinal tract conditions while the matrix consisting of the plant polysaccharide xyloglucan strongly delayed drug release after coating removal. The hemicellulose xyloglucan consists of a backbone of β-1,4-linked glucose moieties, with variable length sidechains containing mainly galactose and xylose [17], and forms a gummy layer of hydrated xyloglucan at the tablet surface seemingly preventing tablet disintegration and restricting drug release. Upon transfer to the colonic dissolution medium, xyloglucanase, an enzyme of the colonic microbiome, acted as potent drug release trigger by cleaving the xyloglucan backbone, thereby accelerating matrix dissolution and drug release. CCR tablets containing 200 mg of either 5-ASA or caffeine demonstrated minimal drug release in *in vitro* simulated gastric and small intestinal test media and significant acceleration of drug release in the presence of physiologically relevant concentrations of microbial xyloglucanase in the colonic dissolution medium, allowing for complete drug release within the expected colonic transit time in humans.

*In vitro* models developed to best represent physiological conditions – including pH, ionic strength, buffer capacity, osmolality, and bile salts – and considering feeding state [18] are widely used for formulation optimization. However, motility patterns, potential interaction with food components, mechanical impact, and absorptive and secretion processes cannot be appropriately simulated *in vitro*, rendering *in vivo* experiments indispensable for ultimate evaluation of dosage form performance. Both the dog and the pig animal models have been employed in studies assessing novel oral formulations for drug delivery to the colon [19,20]. Dog has been the most commonly employed animal model for formulation development [21,22] offering the possibility to administer commercial-sized peroral drug products [23]. However, high canine gastric pH required usually premedication, yet unrealistically low gastric pH values [23] and too brief duration of pH lowering [24] were reported. Also, while canine colonic transit time is comparable to the one in man, both gastric emptying and small intestinal transit are significantly accelerated [23], hampering the assessment of time-dependent colonic release systems. Further, small intestinal length is approximately half of that in man [23], potentially affecting drug absorption processes, and pressure along the upper gastrointestinal tract is strongly increased in beagle dogs [23], influencing drug release from pressure-sensitive formulations such as swollen matrix tablets [21]. Furthermore, dogs are unsuited animal models for 5-ASA formulation assessment due to their differing biotransformation to that in man [25]. Pigs, on the other hand, are increasingly used as preclinical animal model [26–28], as they share a number of anatomical and physiological characteristics with humans for each section of the gastrointestinal tract [28]. Porcine gastric, small intestinal and large intestinal pH and pressure patterns are comparable to those measured in man [29,30] while transit time especially of the large intestine is highly variable in both species and highly dependent on food intake. Moreover, the digestive capacity of porcine and human colonic microbiome have been reported to be similar [31] by virtue also of the omnivorous attitude of pigs, which is relevant for the assessment of microbiome-triggered formulations. The highly variable gastric retention of large monolithic dosage forms, which appears to be prolonged in pigs when compared to man [29,30,32,33], may be the major limitation of the pig model. However, gastric emptying in pigs is still insufficiently characterized, requiring standardized protocols with a large study population [27].

Scintigraphy is used as the standard method to non-invasively determine *in vivo* gastrointestinal transit times and tablet disintegration location. Scintigraphy studies in pigs, however, were hampered by the ambiguous delimitation of small and large intestinal segments [34,35]. Clinical studies were conducted using pharmacokinetics [3], scintigraphy [36,37], or a combination of both [8,9,38] for performance evaluation of peroral colonic drug delivery formulations. In some cases, drug appearance in plasma was earlier than the initial formulation disintegration [8], and differences in tablet disintegration did not always reflect pharmacokinetic profiles [38]. Hence, a combination of scintigraphy for disintegration visualization with pharmacokinetic data may be necessary for ultimate formulation assessment.

The aim of this work was to demonstrate specific colonic delivery with the optimized CCR tablets in an *in vivo* study using the pig as an animal model. CCR tablets were administered to female domestic pigs, drug and metabolite plasma levels were monitored over 96 h after tablet administration and drug recovery in the feces was measured. Intravenous (iv) injection solutions and immediate release (IR) tablets were administered as reference and used to determine pharmacokinetic parameters. Formulation transit through the intestinal tract was described by physiologically based pharmacokinetic modeling (PBPK) and model-bound deconvolution was employed to estimate drug release rate from the CCR tablets and drug mass absorbed from small and large intestinal regions as performance indicators of the developed CCR formulation. Tablets with 5-ASA, typically employed in the treatment of IBD, and with the model drug caffeine were evaluated. Whereas 5-ASA absorption reportedly decreases from proximal to distal parts of the intestine [39,40], caffeine is well absorbed throughout the gastrointestinal tract [11,41] and served therefore as comparator. An IR formulation of sulfasalazine producing sulfapyridine in the colon was used to assess small intestinal transit time in pig while transit time, pressure, and pH along the gastrointestinal tract were monitored by telemetry with a SmartPill® capsule. Xyloglucanase activity and microbiome composition in pig cecum and feces were determined to substantiate the developed colonic delivery approach and provide a basis for result translation from pig to man. Finally, pharmacokinetic data collected with CCR tablets containing a combination of caffeine with sulfasalazine were analyzed to further confirm the location of drug release within the intestine.

## 2. Materials and methods

### 2.1. Materials

5-Aminosalicylic acid (5-ASA) was purchased from AK Scientific, Union City, USA. Xyloglucan 3S was ordered from DSM Gokyo food & chemical, Tokyo, Japan. Sulfasalazine was acquired from Molekula GmbH, München, Germany. Kollicoat IR was obtained from BASF, Ludwigshafen am Rhein, Germany. Eudragit® FS 30 D was kindly donated by Evonik, Essen, Germany. Primojel (sodium starch glycolate

type A) was supplied by DFE Pharma, Goch, Germany. Vivapur 101 (microcrystalline cellulose) was purchased from JRS Pharma, Rosenberg, Germany. Magnesium stearate, talc, titanium dioxide and Granulac 200 (lactose monohydrate) were obtained from Hänseler Swiss Pharma, Herisau, Switzerland. Flowlac 100 was ordered from Meggle, Wasserburg am Inn, Germany. Pharmacoat 603 (hydroxypropyl methylcellulose HPMC 3 mPa·s) was acquired from Shin-Etsu, Tokyo, Japan. Calcium chloride, hematin, histidine, iron (II) sulfate heptahydrate, magnesium chloride, vitamin K3, N-Acetyl-5-ASA (Ac-5-ASA), 4-aminosalicylic acid (4-ASA), caffeine, formic acid, theobromine, theophylline, paraxanthine, polyvinylpyrrolidone (PVP) 30, sulfapyridine, triethyl citrate and iron (II, III) oxide black were supplied by Sigma Aldrich, St. Louis, USA. D9-caffeine was purchased from Santa Cruz Biotechnology, Dallas, USA. Methanol was obtained from Fischer Scientific, Waltham, USA. Hydrochloric acid (HCl) 1 M, glycerol, potassium dihydrogen phosphate, ammonium sulphate, L-cysteine (free base), sodium chloride, sodium dihydrogen phosphate dihydrate, sodium hydroxide (NaOH) 32%, tris, vitamin B12, and iron (III) oxide red were supplied by Carl Roth, Karlsruhe, Germany. Iron (III) oxide monohydrate yellow was purchased from Strem Chemicals Inc., Newburyport, USA. NaOH 1.0 M was supplied by Honeywell-Fluka, Charlotte, USA. Phosphoric acid 85% was obtained from Riedel-de-Haën, Seelze, Germany. Phosphate buffered saline (PBS) pH 7.4 was supplied by Thermo Fisher Scientific, Waltham, USA. Xyloglucanase (nominal activity 1000 U/mL) was purchased from Megazyme, Irishtown, Ireland. Salazopyrin® tablets of Pfizer, containing 500 mg sulfasalazine, were bought in a local pharmacy.

### 2.2. Methods

#### 2.2.1. Peroral formulations

Six peroral formulations were prepared for *in vivo* application. Commercial IR Salazopyrin® tablets containing 500 mg sulfasalazine were cut in halves along the breaking groove and placed in a size 000 gelatin capsules (Wepa Apothekenbedarf, Hillscheid, Germany) for facilitated administration to the animals. CCR 5-ASA and CCR caffeine tablets with composition and manufacturing parameters previously reported [16] were employed. IR 5-ASA, IR caffeine, and CCR caffeine-sulfasalazine tablets had core and coating composition that can be taken from Table S1 in supplementary information.

The granulation and tableting process for preparation of CCR 5-ASA and caffeine tablet cores was previously reported [16]. CCR caffeine-sulfasalazine tablets and IR 5-ASA tablets were prepared after a high-shear granulation of the inner phase components with deionized water at a mixer rate of 250 rpm and a chopper rate of 2200 rpm (Diosna, Osnabrück, Germany). IR caffeine tablets were produced by direct compression. After addition of lubricant and – where applicable – disintegrant, tablets containing 200 mg of either 5-ASA or caffeine, or a combination of 150 mg sulfasalazine and 150 mg caffeine, were produced on a single-punch tablet press (Korsch XL 1, Korsch AG, Berlin, Germany) with concave punches having a diameter of 12 mm and a curvature radius of 9 mm. Tablet cores were coated in a drum coater (GMPC 1 Mini-coater, Glatt, Binzen, Germany) with 3.9 to 5.6% weight gain, corresponding to a l-value of 7.1 to 9.9 mg/cm$^2$. IR tablet cores were non-functionally coated with Kollicoat® IR and CCR tablet cores were enteric coated with Eudragit® FS. Anti-tacking agent, pigments, and – where applicable – plasticizer were homogenized in deionized water for 10 min (IKA® T18 basic Ultra-Turrax®, dispersing tool S18N-10G, IKA®, Staufen, Germany) and the suspension was slowly added under stirring to the coating polymer dispersion, and stirring was continued for at least another 30 min. Batch size was 600 g, whereby 150 g tablet cores were filled up with placebo tablets, and coating process parameters are given in Table S3 in supplementary information.

*2.2.1.1. Dissolution testing.* Dissolution experiments of the five tablet formulations took place in an USP 2 paddle apparatus (Sotax AT7, Sotax, Aesch, Switzerland) at 100 rpm paddle speed and 37 ± 0.5 °C media temperature. For the sulfasalazine capsules, the paddle was replaced by a basket.

Dissolution testing of CCR tablets followed the four-stage protocol previously described [16]. IR tablets were measured in 900 mL HCl 0.1 M and capsules containing Salazopyrin® tablet halves were tested in 900 mL 0.1 M $KH_2PO_4$ pH 6.8. Dissolution experiments were continued until tablet disintegration and an increment between measured concentration of consecutive sampling points of generally <1.15% was reached. Samples of 4.6 mL were withdrawn and replaced with an equal amount of fresh media. Sink conditions were ensured during testing of 5-ASA and caffeine tablets, but not for sulfasalazine in IR capsules and CCR caffeine-sulfasalazine tablets. Dissolution experiments were conducted at least in triplicate and results are expressed in % of drug detected in solution normalized to the final measured value in each vessel corresponding to the end of the dissolution process.

Withdrawn caffeine and 5-ASA samples were filtered through a 0.45 μm nylon filter (Infochroma AG, Goldau, Switzerland) and assayed spectrophotometrically (Jasco V-630 Spectrophotometer, Jasco, Tokyo, Japan), at 303 nm for 5-ASA (acid stage) or 331 nm (buffer stages) and at 272 nm for caffeine. No significant loss of drug was observed after filtration while excipients did not interfere at the employed wavelength (data not shown). Unfiltered sulfasalazine samples were assayed at 360 nm, as filtration led to significant drug loss. Drug was quantified using an external calibration in the range of 1–50 μg/mL, 1–24 μg/mL, and 1–16 μg/mL for 5-ASA, caffeine, and sulfasalazine, respectively.

Samples containing both caffeine and sulfasalazine were centrifuged for 15 min at 14000 rpm and 4 °C (Eppendorf centrifuge 5427 R, Eppendorf, Hamburg, Germany) and the supernatant was analyzed by HPLC, after mixing 200 μL sample with 800 μL methanol for xyloglucan precipitation. After centrifugation for 5 min at 21300 *g* (Eppendorf centrifuge 5425 R, Eppendorf, Hamburg, Germany), 100 μL supernatant were mixed with 300 μL solvent A (5% methanol, 95% $H_2O$ with 0.2% (v/v) formic acid),centrifuged for 5 min at 21300 *g*, and 30 μL were injected onto a Spherisorb C6 column (80 Å, 5 μm, 4.6 mm × 150 mm, Waters, Milford, USA) equilibrated in solvent A at a flow rate of 0.75 mL/min. Analytes were eluted with a linear gradient from 0 to 100% solvent B (95% methanol, 5% $H_2O$ with 0.2% (v/v) formic acid) over 11 min. Caffeine and sulfasalazine were detected at 270 and 359 nm, respectively, and quantified by external calibration in the range of 4–1000 μg/mL for each API subjected to the preparation procedures as described for the samples.

#### 2.2.2. Intravenous solutions

Isotonic, isohydric solutions containing 1% *w/v* of either caffeine or 5-ASA were prepared under aseptic conditions in water for injection, and the pH was brought to 7.3–7.4 with 0.5 M NaOH. The composition of the final solutions can be taken from Table S4 in supplementary information. Solutions were filtered consecutively through 0.45 μm and 0.22 μm sterile filter units (Sartorius, Göttingen, Germany) before being dispensed into heat sterilized brown glass vials. The solutions were kept at room temperature and administered to the animals within 16 h from preparation.

Osmolality (Osmomat 3000 freezing point osmometer, Gonotec GmbH, Berlin, Germany) and pH (827 pH Lab, Metrohm, Herisau, Switzerland) were measured in triplicate on the day of solution

preparation. Concentration of filtered samples (0.22 μm mixed cellulose esters, Milles-GS, Merck, Darmstadt, Germany) was determined in triplicate spectrophotometrically at 272 nm for caffeine and 303 nm for 5-ASA within five hours after application to the animals.

### 2.2.3. Telemetry

The SmartPill® GI system was used for monitoring pH, temperature, and pressure along the gastrointestinal tract of the pigs. The recorder was hung centrally over the individual pens at a height of approximately one meter over the ground. After activation, the correct functioning of the SmartPill® capsule pH sensor was checked at pH 1.2, 6.0, and 9.0.

The MotiliGI® software (Version 3.1.0) automatically performs a temperature compensation of pH and pressure values and applies a baseline correction to the latter measurement set. However, no such baseline correction of pressure data was applied in this work in order to capture the increase in baseline pressure upon arrival of the SmartPill® capsule in the colon using temperature compensated pressure values [30]. All datasets were analyzed in RStudio 2021.09.0 (Rstudio, PBC, Boston, USA).

### 2.2.4. In vivo studies

*2.2.4.1. Animals.* The experimental protocol was approved by the cantonal veterinary authority Zurich, Switzerland (License number ZH154/19). Weaned female crossbreeds of Duroc x Piétrain x Landrace pigs ($n = 14$) aged 3 months were sourced from local breeders. The pigs weighed 42 ± 2 kg in the beginning and 48 ± 2 kg at the end of the experiment (average ± standard error, Table S8 in supplementary information).

The animals were transferred to the experimental animal facility two weeks prior to the start of the experiment for acclimatization. During this phase, the pigs were housed in groups of two and trained by using positive conditioning with raisins and applesauce to get them used to the care takers and the handling in the experimental phase, especially the blood sampling. Three days before the start of the experiment the animals were transferred to individual pens with eye and nose contact. Alimentation during the acclimatization time consisted of 1–1.2 kg PBS30 Viva Plus P 25–110 kg complete feed (Granovit AG, Kaiseraugst, Switzerland) per day fed in two portions, and free access to water.

*2.2.4.2. Study protocol.* Experiments lasted for twelve days, from Monday to Friday of the following week. Two animals were used in parallel each time. On the first day, a venous port system was placed in the jugular vein. For this, animals were pre-medicated with azaperone (2 mg/kg), ketamine (20 mg/kg), and atropine (0.01 mg/kg) intramuscularly 30 min prior to surgery and transferred individually to the surgery room. Before anesthesia, a general health check with special attention to the cardiovascular and respiratory system was performed. An intravenous catheter was placed in one ear and anesthesia was induced with propofol iv (0.4–4 mg/kg). Lidocaine spray was used to desensitize the larynx and the trachea was intubated. Anesthesia was maintained with isoflurane (1–3% v/v in oxygen *via* F-circuit), propofol (0.5–1 mg/kg/h), and ketamine (1–3 mg/kg/h). A sterile port system (central venous catheterization set 16 G, 1.7 mm, Arrow International, Reading, USA) was inserted into the jugular vein using the Seldinger technique in an open surgery. The port system was immediately flushed with heparin (300 IU/kg) and secured with resorbable suture material to the tissue in the periphery of the vessel. The incision was closed in three layers. The port system was closed with a safety connector for aspiration (Safsite Valve, SSC 100, B. Braun, Sempach, Switzerland) and secured with a bandage. The surgery wound was regularly checked and the bandage changed if necessary. Buprenorphine iv (0.02 mg/kg) was administered as analgesic once at the beginning of the surgical procedure and once 4–6 h thereafter. Heparin was dosed systemically immediately after surgery and throughout the experiment at 300 IU/kg every 6–8 h. The pigs were allowed to recover in their pens with unchanged feeding regimen.

Test items were administered on the second, the fifth (exceptionally the third) and the eighth day of the experiment (Table S7 in supplementary information). The last meal was given 14 h prior to dosing and was immediately consumed while water was allowed *ad libitum*. The pigs were sedated for dosage form application using ketamine (10 mg/kg) and medetomidine (0.005 mg/kg) iv and were returned to their pens immediately thereafter. Either two tablets, a tablet and an iv injection, or a SmartPill® capsule and a tablet or an iv injection, were administered at once. Dosage forms administered concomitantly contained a different API (5-ASA, caffeine, or sulfasalazine) and were of different type, *i.e.*, CCR or IR or iv. Care was taken to avoid overlapping blood levels of consecutive administrations. The sequence of test item administration differed among the animals and is shown in Table S7 in supplementary information. Peroral forms were applied to the back of the tongue with a balling gun and were pushed into the stomach with a flexible gavage tube (outer diameter 1.5 cm, Hauptner AG, Langenthal, Switzerland). Intravenous solutions were injected into cannulated ear veins (Surflo® iv catheter, Terumo Europe, Leuven, Belgium) as a bolus injection of 15 mL caffeine or 8 mL 5-ASA solution. Animals were able to stably stand and walk typically within 20–60 min after sedation. Fasting continued for another three hours after drug administration while water was available *ad libitum*. Following this, feeding consisted of 1–1.2 kg PBS30 Viva Plus P 25–110 kg complete feed (Granovit AG, Kaiseraugst, Switzerland) per day fed in several portions coordinated with blood sampling.

Blood samples were drawn at predefined time points from the jugular catheter. The first 3 mL were set aside for later reintroduction to the blood circulation. The next 5 mL were placed in heparinized tubes, shaken and immediately centrifuged for 5 min at 3461 *g* (EBA 20, Hettich Zentrifugen, Tuttlingen, Germany). The plasma supernatant and the cell pellet were kept in separate vials at −20 °C until analysis (section 2.2.4.3). After reinjecting the initially drawn 3 mL of blood, 3 mL heparinized saline (50 IU/mL) were injected to rinse and keep the port system filled. In parallel with formulation administration, a feces sample was taken directly from the rectum and kept at room temperature under anerobic conditions until further processing and analysis (section 2.2.4.5).

All droppings were collected from the pens as immediately as possible but at the latest when blood samples were drawn. Droppings samples was visually inspected for defecated tablets, tablet fragments, or the SmartPill® capsule and were subsequently homogenized to a slurry (Moulinex easymax abm1, Moulinex, France) with one to two weight parts of PBS pH 7.4 depending on sample viscosity, and an aliquot was stored at −80 °C until analysis (section 2.2.4.4).

Following the last blood sampling on the twelfth experimental day, the animals were sedated with intravenous ketamine (10 mg/kg) and medetomidine (0.005 mg/kg) before being euthanized by iv administration of pentobarbital (3000–6000 mg). The cecum was surgically removed, and its content divided into 50 mL aliquots and kept at room temperature under anerobic conditions until further processing and analysis (section 2.2.4.5).

*2.2.4.3. Plasma sample analysis.* Samples were thawed at room temperature, shaken, and centrifuged for 5 min at 21300 *g* (Eppendorf centrifuge 5425 R, Eppendorf, Hamburg, Germany). For protein precipitation, 120 μL plasma were mixed with 400 μL methanol containing 130 ng/mL internal standard (D9-caffeine or 4-ASA, final concentration

100 ng/mL). Mixtures were centrifuged for 10 min at 21300 *g*, stored for 2 h at room temperature, and finally filtered over 0.45 μm PTFE filters (Infochroma AG, Goldau, Switzerland).

A Spherisorb C6 column (80 Å, 5 μm, 4.6 mm × 150 mm, Waters, Milford, USA) connected to an Agilent 1100 HPLC system (Agilent, Santa Clara, USA) was used for chromatographic separation at 25 °C. The column was equilibrated in solvent A (5% methanol, 95% $H_2O$ with 0.2% (v/v) formic acid) at a flow rate of 0.5 mL/min. Two μL of sample were injected and analytes were eluted with a linear gradient from 0 to 100% solvent B (95% methanol, 5% $H_2O$ with 0.2% (v/v) formic acid) over 15 min. Analysis was performed with an Agilent 6470 QQQ MS equipped with an AJS-ESI ion source in positive ion mode with a capillary voltage of 3500 V (Agilent, Santa Clara, USA) and MS/MS analysis parameters as summarized in Table S6 in supplementary information.

For quantification, calibration curves in blank pig plasma samples – obtained from a local butcher – spiked with analyte (caffeine, theobromine, theophylline, paraxanthine, 5-ASA, Ac-5-ASA, sulfasalazine, or sulfapyridine) at concentrations between 2.5 and 2500 ng/mL were prepared. Sample preparation procedure followed the one described above for *ex-vivo* samples. Analyte content in samples were determined using the obtained calibration curves and corrected for deviations using the internal standard intensities in the corresponding samples. The analytical quantification limit was 10 ng/mL.

*2.2.4.4. Fecal dropping analysis.* Dropping slurries were thawed and centrifuged for 2 min at 21300 *g* (Eppendorf centrifuge 5425 R, Eppendorf, Hamburg, Germany). Three hundred μL of the supernatant were diluted with 700 μL $H_2O$ containing 215 ng/mL internal standard (D9-caffeine or 4-ASA, final concentration 150 ng/mL) and centrifuged for 5 min at 21300 *g*, and 950 μL of this supernatant were loaded onto a Screen A SPE column (Phenomenex, Torrance, USA) equilibrated in 25 mM Tris-Acetate, pH 7.5 for sample clean-up. Analytes were eluted with 600 μL 25 mM Tris-Acetate, pH 7.5 containing 50% (v/v) methanol. Three hundred μL eluate and 475 μL flowthrough were mixed and centrifuged for 5 min at 21300 *g* before filtration over 0.1 μm PTFE syringe filters (Infochroma, Goldau, Switzerland).

Chromatographic separation, calibration curve in spiked blank feces extracts – obtained from local breeders – and analyte quantification followed the LC-MS/MS method employed for plasma sample analysis as described in section 2.2.4.3.

*2.2.4.5. Xyloglucanase assay in cecal and rectal feces samples.* One part of cecal and rectal feces samples was diluted under anaerobic conditions with two parts of PBS pH 7.4 and 20 mL of this sample-PBS slurry were mixed with 10 mL glycerol as cryoprotectant. These final samples were kept at −20 °C until enzymatic activity assay.

Xyloglucanase activity was determined in quadruplicate by incubating two different sample volumes with xyloglucan in solution and measuring the viscosity reduction of the solution. For this, finally diluted cecum and rectum fecal samples were thawed at room temperature, and 100 or 200 μL of these slurries were transferred to 5 mL of a 1% *w/v* xyloglucan solution at 37 °C prepared in minimal medium consisting of 13.6 g/L $KH_2PO_4$, 0.875 g/L NaCl, 1.125 g/L $(NH_4)_2SO_4$, 0.5 g/L L-cysteine (free base), 1.9 μM hematin, 0.2 mM histidine, 0.1 mM $MgCl_2$, 0.4 mg/L $FeSO_4 \bullet 7\ H_2O$, 1 mg/L vitamin K3 (menadione), 8 mg/L $CaCl_2$, 5 μg/L vitamin B12. The enzymatic reaction was stopped after 20 or 30 min of incubation at 37 °C by adding 200 μL of 18% HCl to the mixture and the viscosity of the sample was determined at room temperature. Viscosity measurement was carried out with a SV-A1 Vibro viscometer (A&D Company, Tokyo, Japan).

The assay was calibrated by incubating 5 mL of a 1% w/v xyloglucan solution in minimal medium with 100 μL xyloglucanase solution with concentrations ranging from 2.5 to 50 mU/mL and following the same protocol as for the cecum and rectum samples. The data points were approximated by an empirical function as described previously [16].

*2.2.4.6. Pharmacokinetic modeling.* The model-independent pharmacokinetic parameters of maximal concentration, $c_{max}$, and time of its occurrence, $t_{max}$, were read directly from the plasma concentration-time profiles. Statistical analysis was performed with a one-way analysis of variance (ANOVA) in Excel (Version 2205, Microsoft, USA) at a level of significance of $p \leq 0.05$.

Plasma concentration data of 5-ASA and caffeine and their respective metabolite were further analyzed using pharmacokinetic modeling as depicted in Fig. 1.

Gastric emptying was treated as a first order process (IR caffeine) or was encompassed in a lag time (CCR 5-ASA, CCR caffeine, IR 5-ASA) reflecting time to reach measurable plasma concentration. Transit through small intestine was described by a succession of $N = 7$ compartments in accordance to PBPK [42] while the large intestine was treated as a single compartment. A first order transfer rate constant of dissolved mass $m_{si}$ between compartments equal to $N/t_{tr}$ was applied. The full dose of IR tablets was assumed to be present in dissolved form immediately after administration. CCR tablets were assumed to pass through the small intestine at a constant velocity within the transit time $t_{tr}$. Drug release from CCR tablets was assumed to be constant throughout small intestinal passage and during large intestinal residence but release rates were allowed to differ between the small and the large intestine. Fecal loss was considered by adjusting the dose with the absolute bioavailability. Pre-systemic metabolism and peripheral compartment distribution of metabolite were applicable only to 5-ASA. For caffeine, the drug fraction pre-systemically metabolized was set equal to zero (fmet = 0). The meaning of symbols in the equations can be taken from the legend of Fig. 1, D denotes iv, IR or CCR dose and F absolute bioavailability.

All measured concentrations were assigned to the actual sampling times. Dose was corrected with the pig body weight (BW) at the time of administration (Table S8 in supplementary information). The term 'caffeine metabolites' denotes the sum of the three individually measured methylxanthines. Plasma concentrations of parent drug and metabolites below the analytical quantification limit of 10 ng/mL were treated as missing values.

The following systems of ordinary differential equations were established based on the pharmacokinetic model (Fig. 1). Eqs. (1) to (3) apply to IR caffeine, Eqs. (4) to (5) apply to IR 5-ASA, Eqs. (6) to (7) apply to CCR caffeine and CCR 5-ASA, and Eqs. (8) to (12) apply to all types of formulations (iv, IR, CCR) and both drug substances.

$$\frac{dm_{st}}{dt} = -k_{ge} \cdot m_{st} \tag{1}$$

$$\frac{dm_{si}(i)}{dt} = \begin{cases} k_{ge} \cdot m_{st} - k_{a,si} \cdot m_{si}\left(i\right) - \dfrac{m_{si}(i)}{t_{tr}/N}, i = 1 \\ \dfrac{m_{si}(i-1)}{t_{tr}/N} - k_{a.si} \cdot m_{si}\left(i\right) - \dfrac{m_{si(i)}}{t_{tr}/N}, i = 2 - N \end{cases} \tag{2}$$

$$\frac{dm_{li}}{dt} = \frac{m_{si}(7)}{t_{tr}/N} - k_{a,li} \cdot m_{li} \tag{3}$$

The following boundary conditions applied at $t = 0$: $m_{st} = F_{API} \bullet D/BW$, $m_{si} = 0$, $m_{li} = 0$

$$\frac{dm_{si}(i)}{dt} = \begin{cases} 0, \left[0, t_{lag}\right) \\ -k_{a,si} \cdot m_{si}(i) - \dfrac{m_{si}(i)}{t_{tr}/N}, \left[t_{lag}, \infty\right) \wedge i = 1 \\ \dfrac{m_{si}(i-1)}{t_{tr}/N} - k_{a,si} \cdot m_{si}(i) - \dfrac{m_{si}(i)}{t_{tr}/N}, \left[t_{lag}, \infty\right) \wedge i = 2 - N \end{cases} \tag{4}$$

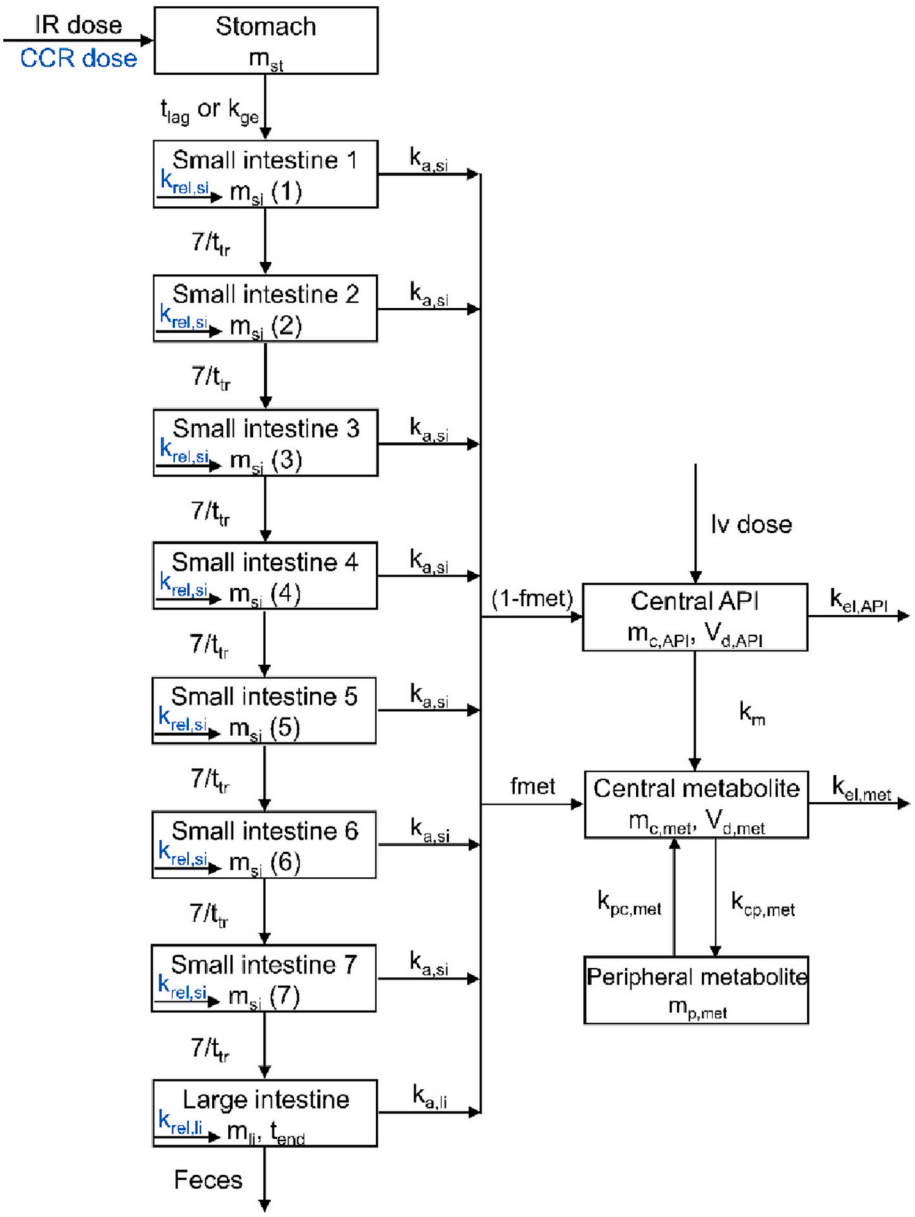


**Fig. 1.** Pharmacokinetic model for *in vivo* data analysis. $m_{st}$, $m_{si}$, and $m_{li}$: dissolved mass in the stomach (gastric), small intestinal (si), and large intestinal (li) compartment, $m_{c,API}$ and $m_{c,met}$: mass of parent drug and metabolite, respectively, in the central compartment, $m_{p,met}$: mass of metabolite in the peripheral compartment, $V_{d,API}$ and $V_{d,met}$: central volume of distribution of parent drug and metabolite, respectively, $k_{ge}$: first order gastric emptying rate constant, $t_{lag}$: lag time, $t_{tr}$: transit time through the small intestine, $t_{end}$: endpoint of drug release from CCR tablets during colonic residence, $k_{rel,si}$ and $k_{rel,li}$ (in blue): zero order drug release rates from CCR tablets in the small and in the large intestine, respectively, $k_{a,si}$ and $k_{a,li}$: first order absorption rate constant from the small and the large intestine, respectively, fmet: drug fraction pre-systemically metabolized, $k_m$: first order metabolic rate constant in the central compartment, $k_{cp,met}$ and $k_{pc,met}$: first order transfer rate constants from central to peripheral and from peripheral to central compartment, respectively, $k_{el,API}$ and $k_{el,met}$: first order elimination rate constant for parent drug and metabolite, respectively. (For interpretation of the references to colour in this figure legend, the reader is referred to the web version of this article.)

$$\frac{dm_{li}}{dt} = \begin{cases} 0, \left[0, t_{lag}\right) \\ \dfrac{m_{si}(7)}{t_{tr}/N} - k_{a,li} \cdot m_{li}, \left[t_{lag}, \infty\right) \end{cases} \tag{5}$$

The following boundary conditions applied at $t = t_{lag}$: $m_{si}(1) = F_{API+met} \bullet D/BW$, $m_{si}(2-N) = 0$, $m_{li} = 0$

$$\frac{dm_{si}(i)}{dt} = \begin{cases} 0, \left[0, t_{lag}\right) \\ k_{rel,si} - k_{a,si} \cdot m_{si}(i) - \dfrac{m_{si}(i)}{t_{tr}/N}, \left[t_{lag}, \left(t_{lag} + \dfrac{i \cdot t_{tr}}{N}\right)\right) \wedge i = 1 \\ -k_{a,si} \cdot m_{si}(i) - \dfrac{m_{si}(i)}{t_{tr}/N}, \left[\left(t_{lag} + \dfrac{i \cdot t_{tr}}{N}\right), \infty\right) \wedge i = 1 \\ \dfrac{m_{si}(i-1)}{t_{tr}/N} + k_{rel,si} - k_{a,si} \cdot m_{si}(i) - \dfrac{m_{si}(i)}{t_{tr}/N}, \left[\left(t_{lag} + \dfrac{(i-1) \cdot t_{tr}}{N}\right), \left(t_{lag} + \dfrac{i \cdot t_{tr}}{N}\right)\right) \wedge i = 2 - N \\ \dfrac{m_{si}(i-1)}{t_{tr}/N} - k_{a,si} \cdot m_{si}(i) - \dfrac{m_{si}(i)}{t_{tr}/N}, \left[t_{lag}, \left(t_{lag} + \dfrac{(i-1) \cdot t_{tr}}{N}\right)\right) \wedge \left[\left(t_{lag} + \dfrac{i \cdot t_{tr}}{N}\right), \infty\right) \wedge i = 2 - N \end{cases} \tag{6}$$

$$\frac{dm_{li}}{dt} = \begin{cases} 0, \left[0, t_{lag}\right) \\ \frac{m_{si}(7)}{t_{tr}/N} - k_{a,li}\cdot m_{li}, \left[\, t_{lag}, \left(t_{lag} + t_{tr}\right)\right) \wedge \left[\, \left(t_{lag} + t_{tr} + t_{end}\right), \infty\right) \\ k_{rel,li} + \frac{m_{si}(7)}{t_{tr}/N} - k_{a,li}\cdot m_{li}, \left[\left(t_{lag} + t_{tr}\right), \left(t_{lag} + t_{tr} + t_{end}\right)\right) \end{cases} \quad (7)$$

The following boundary conditions applied at $t = t_{lag}$: $m_{si}(i) = 0$, $m_{li} = 0$

For model fitting of the IR data, the average value of total clearance of parent drug (Eq. (15)) obtained from the iv experiments was used as a constant in the optimization. The absolute bioavailability for caffeine ($F_{API}$) and 5-ASA ($F_{API+met}$) was estimated from the individual AUC of IR administration data of each animal with reference to the average AUC of iv administration according to Eq. (17). For 5-ASA in particular, the fraction of dose that was systemically metabolized ($k_m/(k_m + k_{el,API})$, Eq. (16)) was assumed to be equal to 0.8 based on literature reports, taking also into account species differences as well as dose-dependent metabolism [44–46]. The expression of elimination and distribution parameters given by Eq. (18) was calculated *a priori* from the ratio of AUC between API and metabolite of the IR administration individually for each experiment and the value obtained was used as a constant in the optimization.

$$\frac{dm_{c,API}}{dt} = \begin{cases} 0, \left[0, t_{lag}\right) \\ (1 - fmet)\cdot \sum_{i=1}^{N} k_{a,si}\cdot m_{si}(i) + (1 - fmet)\cdot k_{a,li}\cdot m_{li} - k_m\cdot m_{c,API} - k_{el,API}\cdot m_{c,API}, \left[\, t_{lag}, \infty\right) \end{cases} \quad (8)$$

$$\frac{dm_{c,met}}{dt} = \begin{cases} 0, \left[0, t_{lag}\right) \\ fmet\cdot \sum_{i=1}^{N} k_{a,si} \bullet m_{si}(i) + fmet\cdot k_{a,li}\cdot m_{li} + k_m\cdot m_{c,API} - k_{el,met}\cdot m_{c,met} - k_{cp,met}\cdot m_{c,met} + k_{pc,met}\cdot m_{p,met}, \left[\, t_{lag}, \infty\right) \end{cases} \quad (9)$$

$$\frac{dm_{p,met}}{dt} = \begin{cases} 0, \left[0, t_{lag}\right) \\ k_{cp,met}\cdot m_{c,met} - k_{pc,met}\cdot m_{p,met}, \left[\, t_{lag}, \infty\right) \end{cases} \quad (10)$$

$$c_{c,API} = \frac{m_{c,API}}{V_{d,API}} \quad (11)$$

$$c_{c,met} = \frac{m_{c,met}}{V_{d,met}} \quad (12)$$

The following boundary conditions applied at $t = 0$: $m_{c,API} = D/BW$ (for iv); at $t = t_{lag}$: $m_{c,API} = 0$ (for IR and CCR), $m_{c,met} = 0$, $m_{p,met} = 0$.

For iv injections, $t_{lag}$, $k_{a,si}$, $k_{a,li}$, and fmet were equal to 0. For IR caffeine, $t_{lag} = 0$.

The system of Eqs. (8) to (12) with either Eqs. (1) to (3) for IR caffeine, or Eqs. (4) and (5) for IR 5-ASA, or Eqs. (6) and (7) for CCR 5-ASA and CCR caffeine was fitted to individual measured plasma concentration data following numerical solution using least square-based regression analysis (EasyFit® 5.12, K. Schittkowski, Germany) [43]. $V_{d,API}$, $V_{d,met}$, $k_{ge}$, $t_{lag}$, $t_{end}$, $k_{rel,si}$, $k_{rel,li}$, $k_{a,si}$, $k_{a,li}$, fmet, $k_m$, $k_{el,API}$, $k_{el,met}$, $k_{cp,met}$, and $k_{pc,met}$ were treated as adjustable parameters. Area under the curve (AUC) was calculated by numerical integration of fitted plasma concentration-time curves until the relative increase of AUC was <0.1% (Eqs. (13) and (14)). All reported values represent average ± standard error of individual experiments.

$$AUC_{API} = \int_0^{\infty} c_{c,API}\cdot dt \quad (13)$$

$$AUC_{met} = \int_0^{\infty} c_{c,met}\cdot dt \quad (14)$$

$$Cl_{API} = \left(k_m + k_{el,API}\right)\cdot V_{d,API} \quad (15)$$

$$Cl_{met} = \frac{D_{iv}}{AUC_{met,iv}}\cdot\frac{k_m}{k_m + k_{el,API}} \quad (16)$$

$$F_{API} = \frac{AUC_{API,IR}\cdot D_{iv}}{AUC_{API,iv}\cdot D_{IR}} \text{ or } F_{API} = \frac{AUC_{API,CCR}\cdot D_{iv}}{AUC_{API,iv}\cdot D_{CCR}}$$
$$F_{API+met} = \left(\frac{AUC_{API,IR}}{AUC_{API,iv}} + \frac{AUC_{met,IR}}{AUC_{met,iv}}\cdot\frac{k_m}{k_m + k_{el,API}}\right)\cdot\frac{D_{iv}}{D_{IR}} \text{ or } F_{API+met} = \left(\frac{AUC_{API,CCR}}{AUC_{API,iv}} + \frac{AUC_{met,CCR}}{AUC_{met,iv}}\cdot\frac{k_m}{k_m + k_{el,API}}\right)\cdot\frac{D_{iv}}{D_{CCR}} \quad (17)$$

$$\frac{AUC_{API}}{AUC_{met}} = \frac{V_{d,met}\cdot k_{el,met}}{V_{d,API}}\cdot\frac{1 - fmet}{fmet\cdot\left(k_m + k_{el,API}\right) + k_m\cdot(1 - fmet)} \quad (18)$$

$$m_{abs,si} = \int_0^{\infty} \sum_{i=1}^{N} k_{a,si}\cdot m_{si}(i)\cdot dt \quad (19)$$

$$m_{abs,li} = \int_0^{\infty} k_{a,li}\cdot m_{li}\cdot dt \quad (20)$$

The estimated values of drug release rates from CCR tablets, $k_{rel,si}$ and $k_{rel,li}$, and the quantities $m_{abs,si}$ and $m_{abs,li}$ calculated by numerical integration of Eqs. (19) and (20) and expressing the drug amount absorbed from the small and the large intestine, respectively, were

obtained by the deconvolution process and were employed as performance indicators of the developed CCR formulation.

## 3. Results

### 3.1. In vitro characterization of applied formulations

Drug release profiles of CCR 5-ASA and CCR caffeine tablets were previously reported [16]. *In vitro* release profiles of IR 5-ASA and caffeine tablets, and IR sulfasalazine capsules, are shown in Fig. S1 in supplementary information. All three IR formulations released >85% of their respective dose within 15 min, and complete dose dissolution was measured within 30 min.

API release from the CCR caffeine-sulfasalazine tablet (in combination) was slightly slower than from CCR caffeine and 5-ASA tablets for 1 U/mL xyloglucanase concentration in the colonic test stage (Fig. S2 in supplementary information), whereby sulfasalazine showed a somewhat larger delay than caffeine. Complete drug dissolution was measured after 9 to 11 h in the colonic dissolution stage.

Table S5 in supplementary information summarizes characteristics of the iv solutions. Osmolality (300–310 mOsm/kg) and pH values (7.3–7.4) were comparable for both drug substances and API content ranged from 101.1 to 104.3% after overnight storage at room temperature.

### 3.2. Pharmacokinetic analysis of caffeine and 5-ASA formulations

Plasma concentration profiles as a function of time of parent drug and main metabolites as well as the corresponding fitted curves are shown in Fig. 2, Fig. 3, Fig. 4, Fig. 5, Fig. 6, and Fig. 7.

Table 1 summarizes deduced pharmacokinetic parameters. Goodness of fit [43] for caffeine and its metabolites was >0.97 after IR and > 0.98 after CCR administration. For Ac-5-ASA, goodness of fit was >0.90 and > 0.92 after IR and CCR administration, respectively. Complete lists of average deduced parameter values for each formulation can be taken from Table S9, Table S10, Table S11, Table S12, Table S13, and Table S14 in supplementary information. A representative profile of deconvoluted caffeine absorption over time after administration of an IR and of a CCR tablet is shown in Fig. S3 in supplementary information.

Caffeine clearance obtained from iv data (Fig. 2) was 0.0341 ± 0.002 L/kg/h (Table S9 in supplementary information). Caffeine metabolites appeared delayed in plasma with a $t_{max}$ of 19 ± 3 h and showed a rather slow elimination.

Gastric emptying rate constant after IR caffeine tablet administration (Fig. 3) was 2.90 ± 1.26 $h^{-1}$ and $k_{a,si}$ was estimated to 4.5 $h^{-1}$ (Table S10 in supplementary information). The ratio of AUC between API and metabolites amounted to 2.37 ± 0.27. IR caffeine tablets gave an absolute systemic bioavailability, $F_{API}$, of 77.4 ± 5.7%. Time until maximal plasma concentration, $t_{max}$, was 2.7 ± 0.8 h for caffeine and 16.5 ± 2.4 h for the metabolites. Almost 100% of caffeine absorption was estimated to take place from the small intestine, and total calculated absorbed mass was in perfect agreement with measured bioavailability values (Table 1).

In comparison to IR, CCR caffeine tablets (Fig. 4) yielded a significantly increased $t_{max}$ ($p \leq 0.001$) and a significantly reduced $c_{max}$ ($p \leq 0.001$) (Table 1). A lag time, $t_{lag}$, of 2.1 ± 0.6 h (Table S11 in supplementary information) was found for CCR caffeine tablets. The ratio of AUC between API and metabolites was 2.17 ± 0.22 (Table S11 in supplementary information). CCR caffeine tablets showed an absolute bioavailability of 58.2 ± 6.2%, corresponding to 75% relative bioavailability when compared to the IR administration. Roughly 96% of caffeine absorption for CCR tablets was estimated to take place in the large intestine. Deduced mass absorbed from the small intestine was significantly ($p \leq 0.001$) smaller for CCR compared to IR caffeine tablet administration. Total calculated absorbed mass was in perfect agreement with measured bioavailability values. Deduced caffeine release rate from the CCR tablets was significantly larger in the large intestine than in the small intestine ($k_{rel,li}$ = 30.9 µmol/h and $k_{rel,si}$ = 9.8 µmol/h, respectively, $p \leq 0.05$). The relative standard deviation of the individual estimates [43] from model fitting to data of each animal varied between 0.1 and 8% for $k_{rel,li}$ and between 3 and 71% for $k_{rel,si}$. Release was estimated to terminate 19.9 ± 2.2 h after colonic arrival of the tablet.

After iv 5-ASA administration (Fig. 5), metabolite appearance in plasma was very rapid with $t_{max}$ values coinciding with that of parent drug, in line with human data after low dose application of 100 or 250 mg, whereas saturation of acetylation and slower metabolite formation has been shown at higher doses [44,45]. Clearance of parent drug 5-ASA and main metabolite Ac-5-ASA obtained from iv data modeling was 2.80

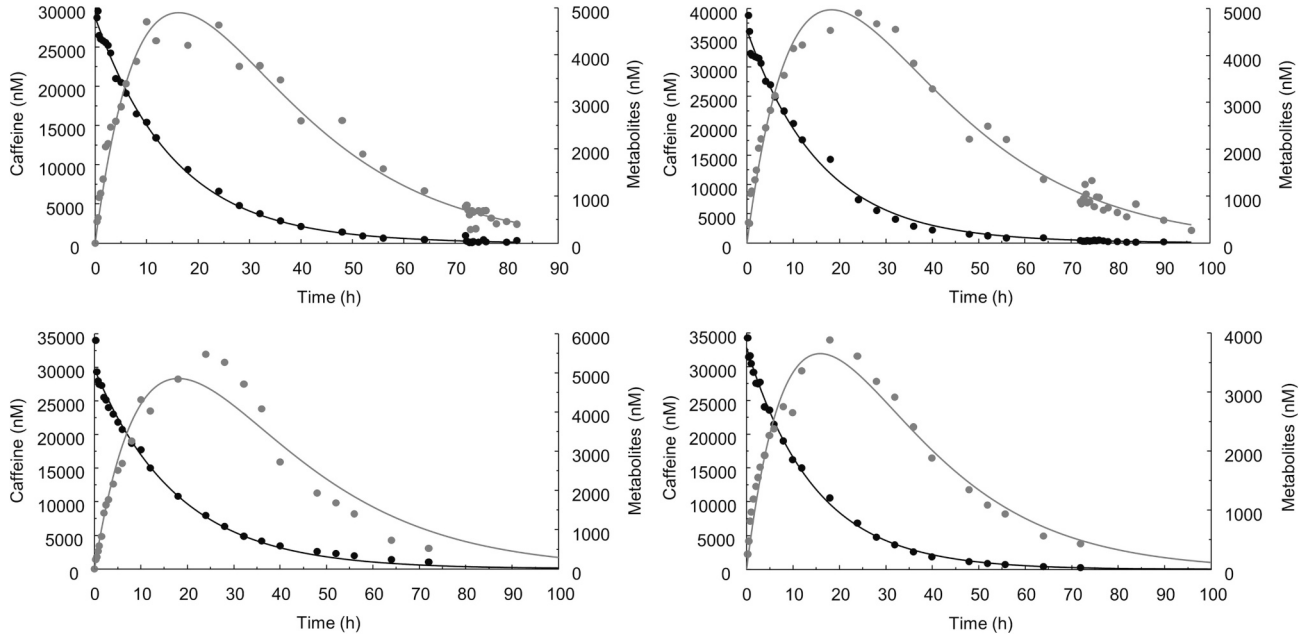


**Fig. 2.** Individual plasma concentration profiles after iv caffeine administration as a function of time for parent drug (black) and metabolites (grey). Points represent measured data and lines fitted model functions.

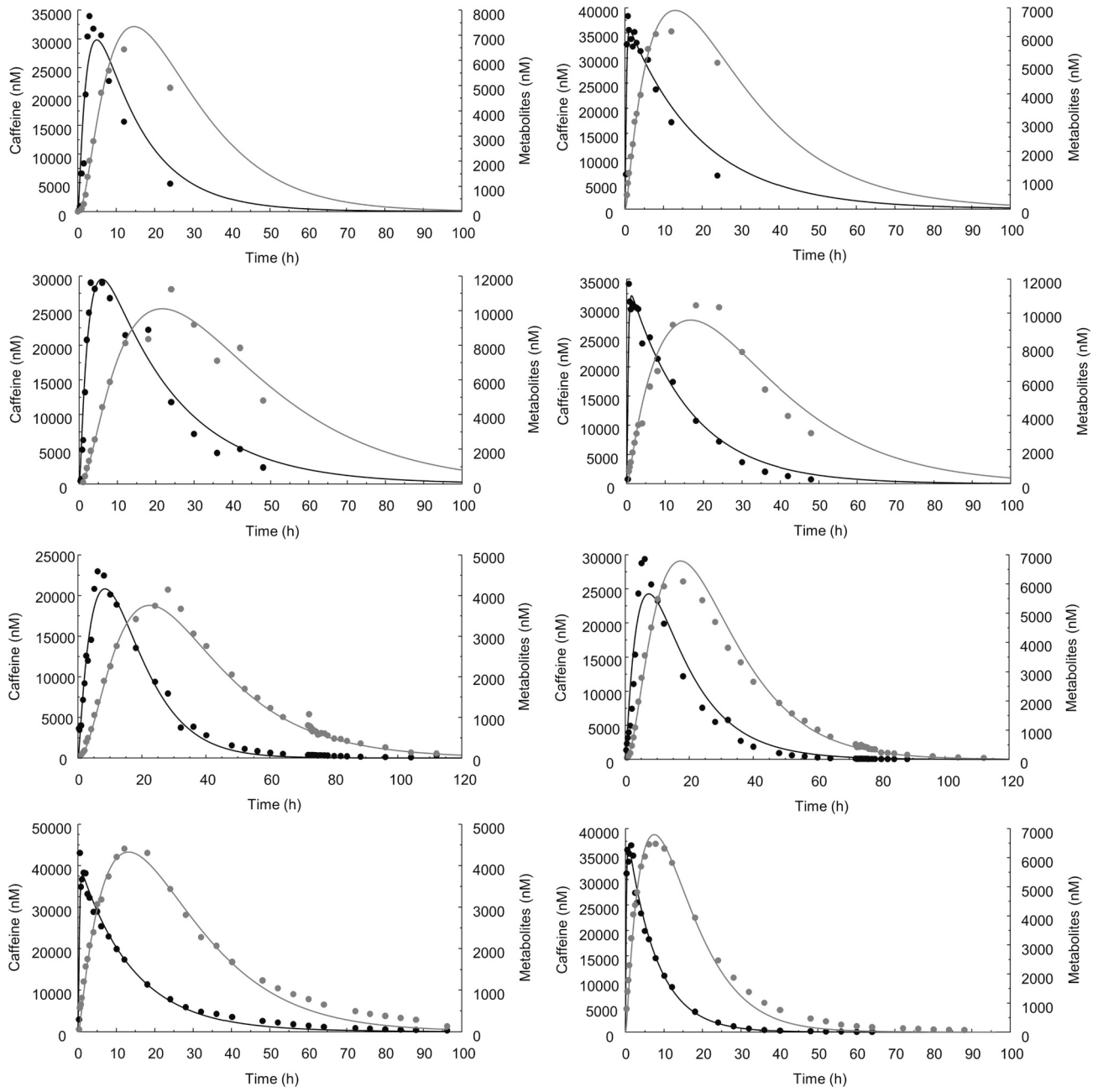


**Fig. 3.** Individual plasma concentration profiles after IR caffeine tablet administration as a function of time for parent drug (black) and metabolites (grey). Points represent measured data and lines fitted model functions.

± 0.40 and 0.64 ± 0.04 L/kg/h, respectively (Table S12 in supplementary information), whereby the fraction that was systemically metabolized was set equal to 0.8 [44–46].

Delayed plasma appearance after IR 5-ASA tablet application (Fig. 6) was measured with a $t_{lag}$ of 2.3 ± 0.5 h. The small intestinal absorption rate constant was estimated to be 2.96 ± 1.44 $h^{-1}$. A significant pre-systemic metabolism of 92 ± 3% was found (Table S13 in supplementary information) and parent drug plasma concentrations remained below analytical quantification limit throughout sampling time in three animals. Wherever measurable, $t_{max}$ of parent drug was identical to that of metabolite. The ratio of AUC between API and metabolite was equal to 0.025 ± 0.011 (Table S13 in supplementary information). Systemic absolute bioavailability considering parent drug and its main metabolite, $F_{API+met}$, amounted to 67.0 ± 7.2%. Absorption was estimated to take place from both the small and the large intestine, contrasting the caffeine results. Total calculated absorbed mass was in perfect agreement with measured bioavailability values.

Comparison between IR and CCR 5-ASA parameters was based on the main metabolite Ac-5-ASA as justified by the coinciding $t_{max}$ of parent drug and metabolite and in accordance with previous *in vivo* experiments [8], since CCR 5-ASA tablets gave plasma concentration of parent drug mostly below the limit of analytical quantification (Fig. 7). A lag time of 2.7 ± 0.8 h (Table S14 in supplementary information) was found. CCR 5-ASA tablets gave a significantly increased $t_{max}$ ($p \leq 0.01$) and a significantly reduced $c_{max}$ ($p \leq 0.05$) when compared to the IR formulation (Table 1). Absolute bioavailability of CCR 5-ASA tablets amounted to 42.2 ± 8.8%, corresponding to 63% relative bioavailability when compared to the IR formulation. Because of the unquantifiable plasma levels of 5-ASA, the average values of the pre-systemic metabolism fraction, fmet, and of the expression given by Eq. (18) obtained

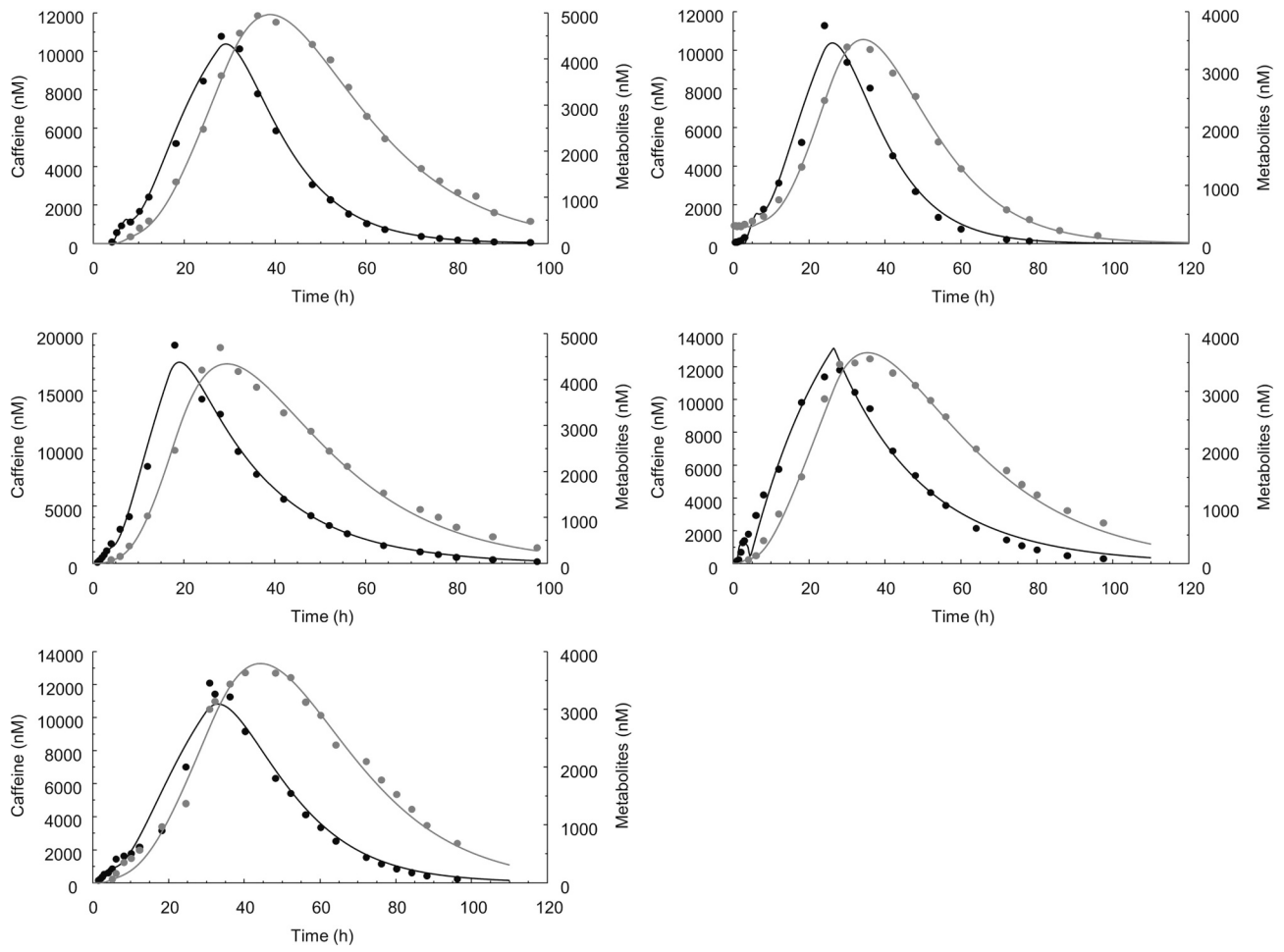


**Fig. 4.** Individual plasma concentration profiles after CCR caffeine tablet administration as a function of time for parent drug (black) and metabolites (grey). Points represent measured data and lines fitted model functions.

from the IR 5-ASA experiments were used as constants in model fitting of the CCR 5-ASA data. A much larger mass was estimated to be absorbed in the large intestine compared to the small intestine and deduced absorption from the small intestine was smaller for CCR tablets than for IR tablets, these model-based estimates for the CCR 5-ASA tablets, however, are interpreted only as trends and no reliable estimation of 5-ASA release rates was possible due to the mentioned adoption of the IR values in the CCR fitting operation and because of the small number of available plasma concentration data points leading to over-parametrization. Release from CCR 5-ASA tablets was found to terminate 7.7 ± 1.4 h after colonic arrival. Compared to CCR caffeine tablets, CCR 5-ASA formulations showed a shorter release duration after colonic arrival, and a lower bioavailability.

Full agreement of calculated total absorbed masses with measured absolute bioavailability values endorsed pharmacokinetic model validity for all formulations with the exception of CCR 5-ASA, probably because the used fmet and Eq. (18) values were under- and over-estimated, respectively (see above).

### 3.3. Pharmacokinetic analysis of sulfasalazine formulations

#### 3.3.1. IR sulfasalazine

Plasma concentration profiles of sulfasalazine, a diazo prodrug, sulfapyridine cleaved from sulfasalazine by azoreductases in the large intestine [12], and the metabolite Ac-5-ASA are displayed in Fig. S4 in supplementary information. The onset of measurable plasma concentration of sulfapyridine was noted 2 to 3 h after tablet administration. The 5-ASA plasma concentration remained below quantification level throughout the experiment.

#### 3.3.2. CCR caffeine-sulfasalazine

Plasma concentration profiles of caffeine and sulfasalazine as well as their respective metabolites after co-administration with the same tablet are displayed in Fig. S5 in supplementary information. The 5-ASA plasma concentration remained below quantification level. The onset of measurable plasma concentration was noted 6 to 8 h for sulfapyridine and 2 to 5 h for caffeine after tablet administration. Time to reach maximal plasma concentrations, $t_{max}$, was practically identical for these two substances in two out of three experiments and the terminal segments of their plasma profile were parallel indicating comparable elimination behavior (Fig. 8).

### 3.4. Caffeine, 5-ASA, and metabolite content in fecal droppings

Amount of parent drug and metabolites recovered in droppings after administration of peroral caffeine and 5-ASA dosage forms is shown in Fig. 9. Despite the practical difficulty of quantitatively collecting fecal droppings from the pens, leading inevitably to uncertainty, these results reveal clear trends. Predominately the metabolite Ac-5-ASA was found in droppings and its cumulative amount represented a large proportion of the 5-ASA dose administered with the tablets. For caffeine, an overall small amount of the parent drug and no metabolites was recovered. No clear difference between IR and CCR administration was detected in terms of fecal recovery.

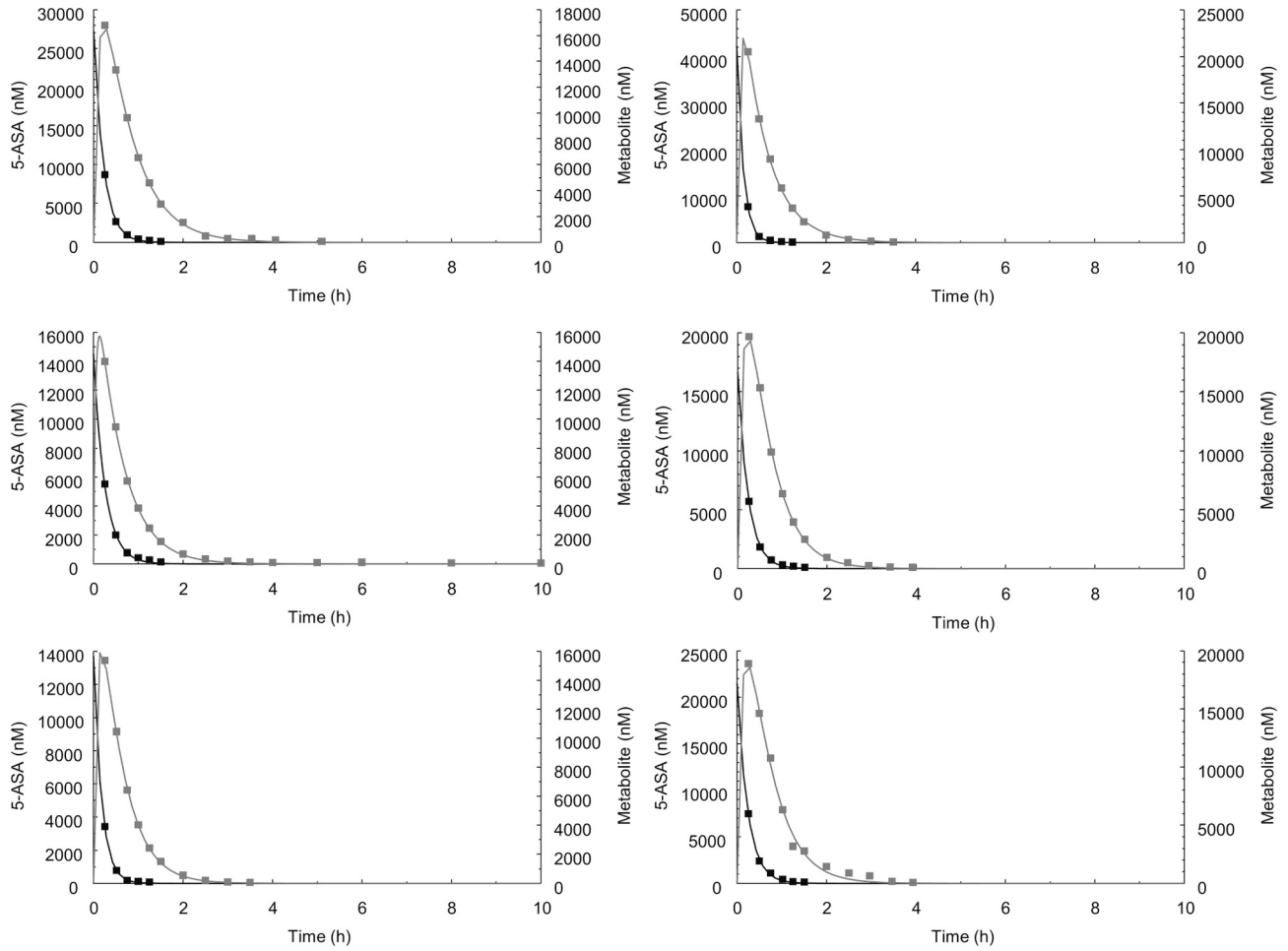


**Fig. 5.** Individual plasma concentration profiles after iv 5-ASA administration as a function of time for parent drug (black) and metabolite (grey). Points represent measured data and lines fitted model functions.

### 3.5. Xyloglucanase activity

Average xyloglucanase activity measured in rectal samples and, after euthanasia, in cecum samples is shown in Fig. 10. The average (± SE) enzyme activity over all rectal samples was 280 (± 38) mU/g ranging from 22 to 1210 mU/g while the average value in cecum was 35 (± 4.6) mU/mL ranging from 13 to 69 mU/mL (Fig. S6 in supplementary information). Values of rectal feces samples showed considerable intra- and interindividual variability but no general effect of study time on enzyme activity. For each animal, cecal xyloglucanase activity was lower than the minimal value of the rectal samples.

### 3.6. Telemetry

SmartPill® telemetric capsules were administered to ten animals. Data analysis was possible for nine of them, as one capsule did not transmit any data. The results of pH, temperature, and pressure are shown in Fig. S7 in supplementary information. Capsule ingestion was detected by an abrupt temperature increase from room to physiological body temperature. Gastric emptying was identified by a sharp pH rise of at least three units. Colonic arrival time corresponding to the ileocecal junction was detected by a sudden pH decrease of more than one pH unit and small intestinal transit time was calculated as the difference between colonic arrival and gastric emptying time. Capsule excretion was detected by either visual recovery in feces samples or a sharp temperature drop, and the whole gut transit time was determined as the time from ingestion to excretion [21]. Individual transit times are summarized in Table 2.

Gastric emptying time of the telemetric capsule was long and highly variable and exceeded the battery life of the capsule in four out of nine pigs. Whole gut transit time could be measured for five animals, for which small intestinal transit time ranged from 2.6 to 4.5 h while colonic transit time varied from 18.5 to 62.8 h. Defecation was detected after whole gut transit times of 99.1 to 135.9 h.

No post-run calibration of the pH measurement could be conducted (see section 4.5) because the capsules were either not defecated or had insufficient battery capacity after recovery in the fecal droppings. The observed pH drift was therefore not corrected and only relative changes of measured pH values marking the transition between segments of the gastrointestinal tract were interpreted. The pH profiles showed large variability during gastric residence yet the passage from the stomach to the duodenum and the entry into the ascending colon could be clearly demarcated.

The highest pressure (227 ± 14.5 mbar, $n = 9$) was detected in the stomach. A pressure baseline change occurred between 0 and 3.5 h after colonic arrival.

## 4. Discussion

### 4.1. In vitro formulations analysis

Dissolution testing and drug release from CCR tablets *in vitro* was extensively discussed previously [16]. The slightly lower release rate of caffeine from CCR tablets containing caffeine and sulfasalazine

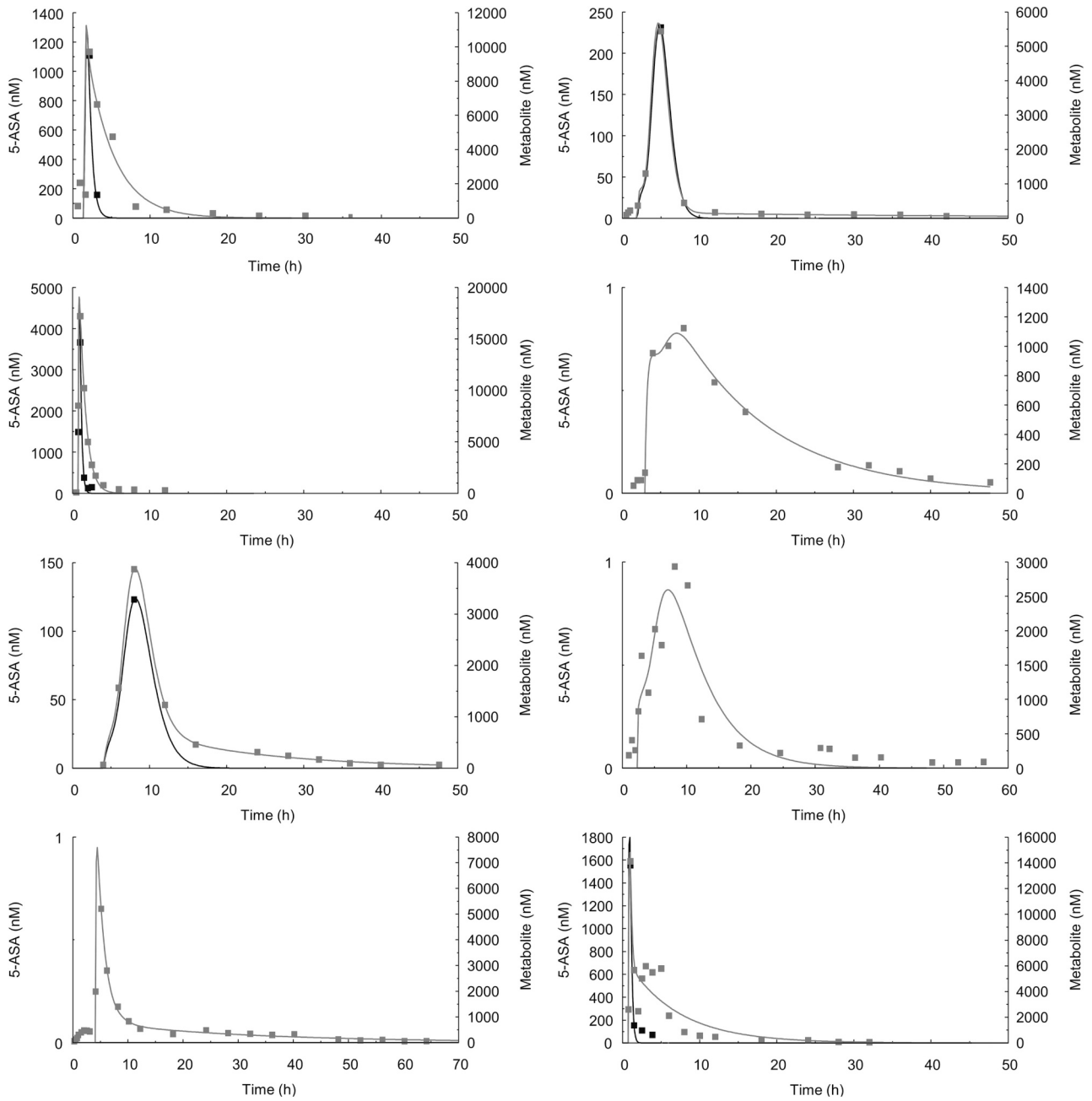


**Fig. 6.** Individual plasma concentration profiles after IR 5-ASA tablet administration as a function of time for parent drug (black) and metabolite (grey). Points represent measured data and lines fitted model functions.

compared to the pure caffeine CCR tablets is probably because of the different granulation methods used, producing higher density particles by high shear granulation in the former compared to fluidized bed granulation in the latter ([16] and Table S2 in supplementary information). Sulfasalazine release was slower than caffeine release under colonic test conditions which was probably because of the lower solubility and the non-sink measurement conditions of sulfasalazine [47,48] compared to caffeine [49].

Release characteristics of IR caffeine and 5-ASA formulations were confirmed in gastric dissolution media while capsules containing Salazopyrin® tablet halves showed IR characteristics when tested in intestinal media confirming the absence of influence of the manipulation of the commercial product on dissolution. Testing was carried out in intestinal media because of the poor solubility of sulfasalazine in acidic pH [48].

### 4.2. Modeling and basic pharmacokinetic parameters

Release rates of CCR tablets and absorbed drug quantities from small and large intestine for IR and CCR tablets were estimated from measured plasma concentration profiles by deconvolution based on fitting of the PBPK model. Parent drug and metabolite data were both used in the model, as plasma concentrations of 5-ASA were highly variable and mostly not quantifiable when CCR tablets were administered. Results of each animal were modeled individually and average values with standard errors of estimated parameters are reported to convey a sense of interindividual variability. Average API clearance from the iv experiments and an expression of disposition parameters (Eq. (18)) of each individual animal experiment were used as constants in model fitting of the data of the respective experiment to provide stability of optimization, since no randomized cross-over study design was employed. Both

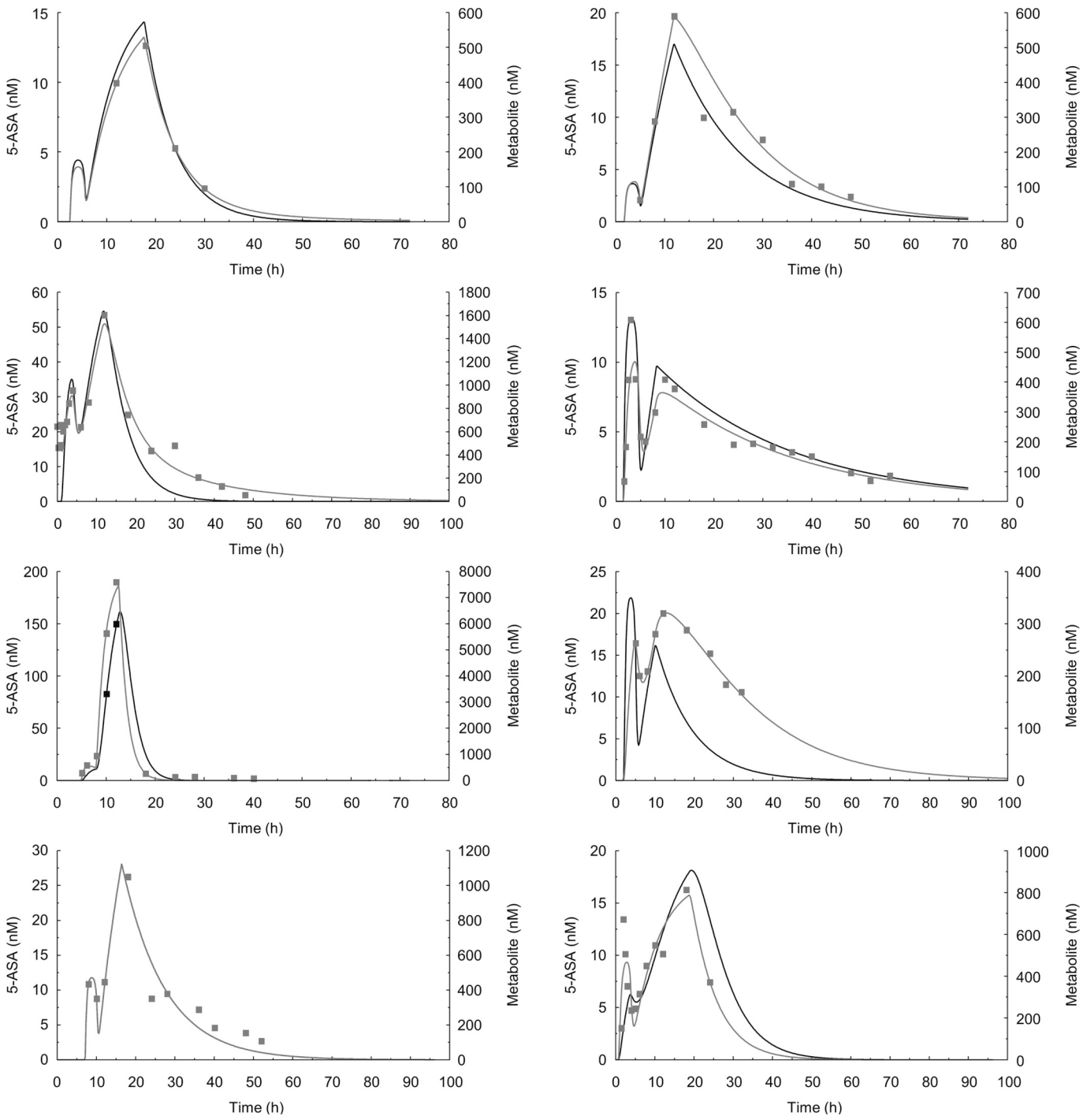


**Fig. 7.** Individual plasma concentration profiles after CCR 5-ASA tablet administration as a function of time for parent drug (black) and metabolite (grey). Points represent measured data and lines fitted model functions. Parent drug curves are simulated (with one exception) and remain below the limit of analytical quantification.

these quantities exhibited small variability (see Results section). For CCR 5-ASA tablet data, the average value of Eq. (18) calculated from the IR 5-ASA experiments was used as a constant in the optimization because API plasma levels in the former were mostly not quantifiable (see Section 3.2). Dose fraction absorbed in the IR experiments was defined as absolute bioavailability, which in the case of 5-ASA included the metabolite to account for the extensive pre-systemic metabolism.

First order gastric emptying was appropriate for modeling IR caffeine but not IR 5-ASA data. Sedation, necessary for drug administration, did not seem to affect gastrointestinal motility of the pigs, as demonstrated by the rapid plasma appearance of drug after IR caffeine administration. To estimate first order small intestinal absorption rate constant, $k_{a,si}$, of caffeine, values within a wide range were assigned to this parameter and the value providing the smallest cumulative residuals of the optimization over all experiments was determined. The resulting $k_{a,si}$ value of 4.5 $h^{-1}$ was in the range of reported absorption rate values for caffeine in man [50] while a gastric emptying rate constant and variability thereof were obtained in general agreement with reports about gastric emptying in pigs [29,34,51].

Contrary to caffeine and agreeing with previous work [3], a lag time

**Table 1**
Deduced pharmacokinetic parameters from animal study (mean ± standard error).

| Tablet formulation | Parameter | Caffeine | 5-ASA |
|---|---|---|---|
| IR | Replicates | 8 | 8 |
| | Dose (μmol) | 1030 | 1306 |
| | $t_{max}$ (h) | 2.7 ± 0.8 | 4.8 ± 1.1* |
| | $c_{max}$ (μM) | 33.4 ± 2.2 | 7.5 ± 2.0* |
| | F (%) | 77.4 ± 5.7 | 67.0 ± 7.2** |
| | $m_{abs,si}$ (μmol) | 796 ± 59.0 | 561.6 ± 180.6** |
| | $m_{abs,li}$ (μmol) | 0.2 ± 0.1 | 311.7 ± 107.6** |
| CCR | Replicates | 5 | 8 |
| | Dose (μmol) | 1030 | 1306 |
| | $t_{max}$ (h) | 25.8 ± 2.2 | 13.2 ± 1.8* |
| | $c_{max}$ (μM) | 13.0 ± 1.5 | 1.6 ± 0.9* |
| | F (%) | 58.2 ± 6.2 | 42.2 ± 8.8** |
| | $m_{abs,si}$ (μmol) | 27.3 ± 5.9 | 61.0 ± 15.5**,# |
| | $m_{abs,li}$ (μmol) | 580.1 ± 65.0 | 610.5 ± 146.9**,# |
| | $k_{rel,si}$ (μmol/h) | 9.8 ± 2.1 | – |
| | $k_{rel,li}$ (μmol/h) | 30.9 ± 6.0 | – |

* Based on the drug metabolite Ac-5-ASA.
** Based on the sum of parent drug, 5-ASA, and drug metabolite, Ac-5-ASA.
\# Estimated using fmet and Eq. (18) values of the IR experiment.

was required for modeling plasma profiles of IR 5-ASA tablets. This may be related to the extensive intestinal and liver first-pass metabolism, which is saturable as absorption rate increases [52], in combination with an initially incomplete dissolution of the administered 5-ASA dose in the upper small intestine, lowering the absorption rate. Indeed, 5-ASA solubility is highly pH-dependent and ranges from 1.4 to 9.4 mg/mL [14,53] at physiological pH values in the small intestine considering microenvironmental pH decrease upon 5-ASA dissolution at the given buffer capacity [54]. Dissolution of the administered dose in 100 mL of fluid yields a concentration within this range indicating that saturation might be reached *in vivo*. The employed dose of 200 mg in the 5-ASA tablets, although proven in this work to be too low for facile pharmacokinetic analysis, was chosen in order to be equal to the one of caffeine and allow the manufacture of tablets with identical size, shape, and drug load for both APIs. The determined $k_{a,si}$ value of 2.96 $h^{-1}$ for 5-ASA is comparable to that of caffeine. The large fraction of pre-systemic metabolism, fmet, after peroral 5-ASA administration probably resulted from the comparatively small dose employed and is in agreement with undetectable 5-ASA but substantial Ac-5-ASA plasma levels after IR sulfasalazine administration.

A typical small intestinal transit time of three hours was derived from the time until notable increase in sulfapyridine plasma concentration occurred after peroral administration of IR sulfasalazine (Fig. S4 in supplementary information), in combination with the results of the telemetry measurements (Table 2). This transit time is supported by literature and was reported to show rather small intra- and interindividual variability [10].

The sum of the three caffeine metabolites was used for simplicity in the present pharmacokinetic analysis. Although caffeine metabolism was described to differ between species in terms of variable ratio between the three methylxanthines [55,56] this was not deemed relevant in this study. Nevertheless, reported caffeine clearance is similar for man and pig [57] and comparable to the results of this work. Pharmacokinetics and biotransformation of 5-ASA are identical in man and pig [25].

A two-compartment model provided better goodness of fit of Ac-5-ASA data and has been used for 5-ASA previously [3,39]. For all other molecular species, one compartment model was adequate. The caffeine doses employed in this study displayed linear pharmacokinetics while both linear and dose-dependent pharmacokinetics were presented in the literature [58,59].

### 4.3. Evaluation of colonic delivery

The CCR formulation had a significant impact on model-independent pharmacokinetic parameters $c_{max}$ and $t_{max}$ compared to the IR tablets for both drug substances. The strong increase of $t_{max}$ and accompanying decrease of $c_{max}$ as well as the magnitude and reproducibility of $t_{max}$ (25.8 ± 2.2 and 13.2 ± 1.8 h for caffeine and 5-ASA, respectively) for CCR tablets are viewed as indications of drug absorption taking place from the large intestine. The increase of $t_{max}$ was stronger for caffeine than for 5-ASA. This results, firstly, from the longer $t_{max}$ of IR 5-ASA compared to IR caffeine (4.8 *vs.* 2.7 h, respectively), which is consistent with the lag time of IR 5-ASA of 2.3 h, and secondly from the shorter $t_{max}$ of CCR 5-ASA compared to CCR caffeine. The latter might be attributed to less efficient absorption of 5-ASA in lower regions of the large intestine (see discussion below).

Co-administration experiments of caffeine and sulfasalazine formulated in the same CCR tablet were performed to test the hypothesis of drug absorption for these tablets taking place predominantly in the large intestine. The onset of measured caffeine plasma concentration was the same as the $t_{lag}$ of the pure CCR caffeine tablets and manifested delayed

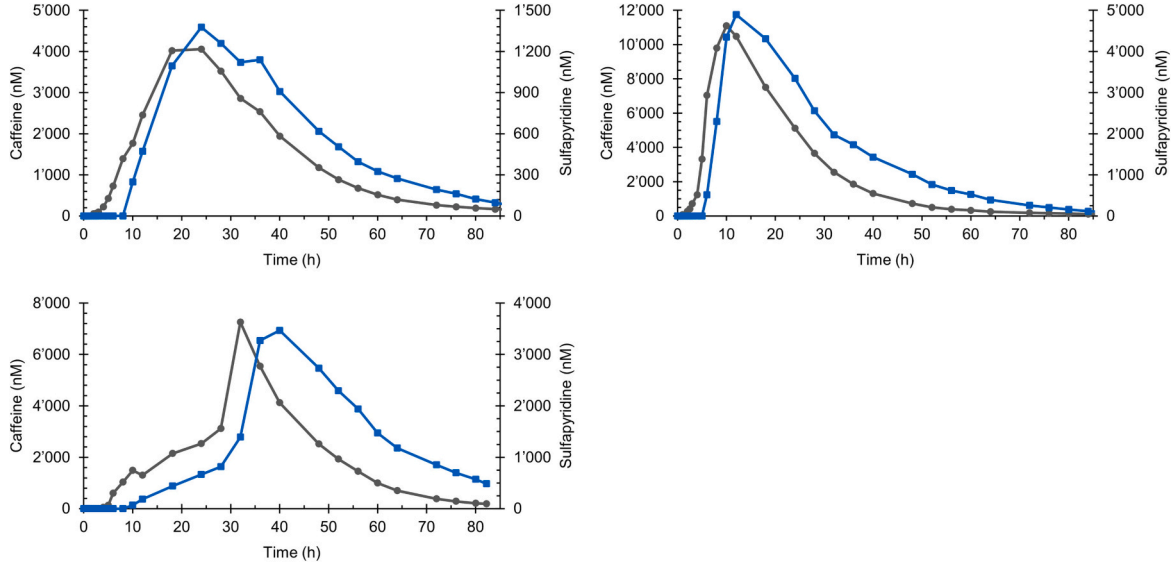


**Fig. 8.** Individual plasma concentration profiles after CCR caffeine-sulfasalazine administration as a function of time for caffeine (grey circles) and sulfapyridine (blue squares). (For interpretation of the references to colour in this figure legend, the reader is referred to the web version of this article.)

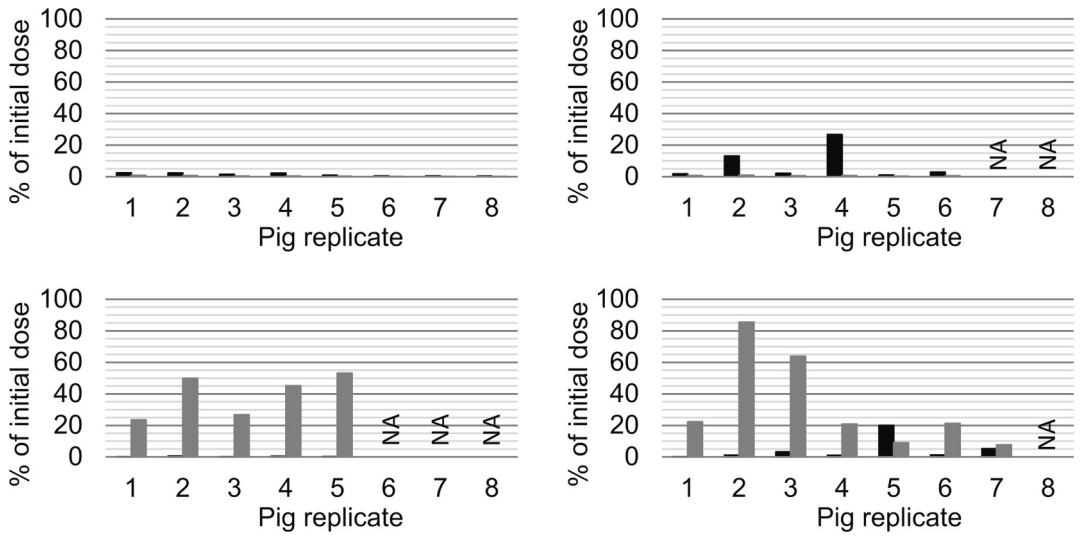


**Fig. 9.** Cumulative recovery of parent drug (black columns) and metabolites (grey columns) in percent of the initial dose in pig droppings after administration of IR caffeine (top left panel), CCR caffeine (top right panel), IR 5-ASA (bottom left panel), and CCR 5-ASA tablets (bottom right panel). NA: Not available.

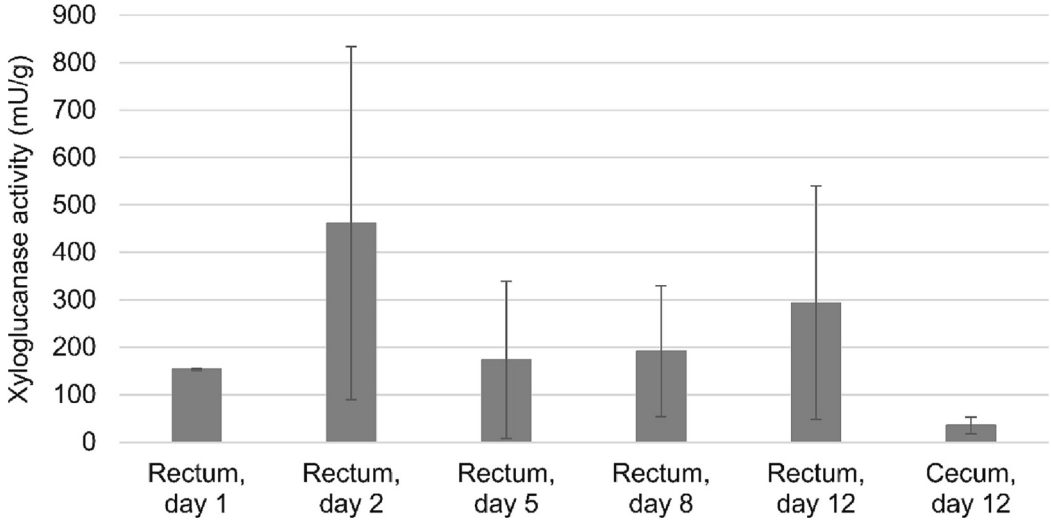


**Fig. 10.** Xyloglucanase activity in rectum and cecum samples of different animals at time points coinciding with dosage form administration. Columns and error bars represent average and standard deviation, respectively ($n = 2$ for day 1, $n = 11$–$14$ for all other time points).

**Table 2**
Individual transit times of a telemetric capsule administered to fasted pigs. GET: gastric emptying time, SITT: small intestinal transit time, CAT: colonic arrival time, CTT: colon transit time, WGTT: whole gut transit time.

| Pig replicate | 1 | 2 | 3 | 4 | 5 | 6 | 7 | 8 | 9 | 10 |
|---|---|---|---|---|---|---|---|---|---|---|
| GET (hh:mm) | 45:57 | >136 | >91 | 44:28 | >84 | 108:53 | – | >124 | 70:00 | 69:18 |
| SITT (hh:mm) | 2:36 | – | – | 3:36 | – | 2:56 | – | – | 4:27 | 3:46 |
| CAT (hh:mm) | 48:33 | – | – | 48:04 | – | 111:49 | – | – | 74:27 | 73:04 |
| CTT (hh:mm) | 50:33 | – | – | 54:10 | – | 18:46 | – | – | 34:24 | 62:47 |
| WGTT (hh:mm) | 99:06 | – | – | 102:14 | – | 130:35 | – | – | 108:51 | 135:51 |

absorption compared to IR tablets. This onset of measured caffeine plasma concentration occurred 3 to 4 h earlier than the one of sulfapyridine which is consistent with the observed delay of sulfapyridine plasma appearance upon administration of the IR sulfasalazine formulation (Fig. S4 in supplementary information). This suggests that after release of caffeine and sulfasalazine from the CCR formulation, sulfapyridine is generated by microbial enzymes [12] upon arrival of released sulfasalazine in the large intestine from where sulfapyridine is subsequently absorbed. Notably, the practically identical $t_{max}$ of the two substances following a steep concentration rise (Fig. 8) indicates that they are absorbed concomitantly and supports the hypothesis that caffeine is absorbed from the large intestine when administered with CCR tablets. One of the CCR caffeine-sulfasalazine co-administration experiments yielded plasma profiles with a different shape of the ascending part that differed also in their $t_{max}$ and were thus inconclusive in this respect invoking the exclusion of such results from further evaluation.

Model-based analysis reveals overwhelming absorption of caffeine

for CCR tablets in the large intestine while absorption of caffeine for IR tablets is calculated to take place practically exclusively in the small intestine (Table 1). Absorption as a function of time for both tablet formulations is depicted in an example in Fig. S3 in supplementary information. These results are consistent with literature reports about good caffeine absorption throughout the gastrointestinal tract [11,41] and the generally rapid absorption of caffeine in man [60]. For CCR 5-ASA tablets, predominant absorption in the large intestine is deduced on account of the metabolite detected in plasma. Decreasing 5-ASA absorption from proximal to distal regions of the gastrointestinal tract has been described [44,52] yet the previously held assumption that 5-ASA exhibits practically no absorption from the colon [61] has been proven inaccurate by sulfasalazine administration experiments, in which 5-ASA was measured in plasma in man [39,62]. In the present work, however, 5-ASA is completely metabolized pre-systemically in the liver. Absorption for IR 5-ASA tablets appears to take place from both the small and large intestine. In view of reports describing rapid 5-ASA absorption from the upper gastrointestinal tract in man [44] this result may be due to slow drug dissolution leading to a lag time (see above) and incomplete dose absorption in the small intestine considering also the small intestinal transit time of three hours employed in the model. Notably, the estimated absorbed mass from the small intestine was significantly smaller for CCR than IR tablets and amounted to 2.6% of the initial caffeine dose and a similarly small percentage of the 5-ASA dose.

Drug release from CCR tablets and drug absorption are modeled as distinct kinetic processes allowing for independent transport of tablet and dissolved drug along the gastrointestinal tract. Absorption from the large intestine practically commences when time exceeds the sum of lag time plus small intestinal transit time given that both drugs are reported to be readily absorbed in the small intestine [44,60] and that the deduced absorption rate constants in the small intestine were large ($k_{a,si}$ = 4.5 $h^{-1}$ and 2.96 $h^{-1}$ for caffeine and 5-ASA, respectively). Therefore, it can be inferred from the present results that drug release from CCR tablets took place predominantly in the large intestine. This data, therefore, provides evidence of controlled colonic delivery. Also, very limited drug release in the small intestine is implied. This underscores the function of the xyloglucan matrix to prevent release after coating dissolution and before tablet entry into the colon. The release delaying function of the coated polysaccharide matrix is further manifested by the increased $t_{lag}$ of the CCR tablets for all tested substances compared to their IR counterparts which is considered to comprise the time until coating dissolution and begin of release from the matrix in the small intestine.

Deduced drug release rate from CCR caffeine tablets *in vivo* was much larger in the large intestine compared to the small intestine (Table 1). The significant increase of release rate in the colon reflects the action of bacterial enzymes on the tablet matrix eliciting hydrolysis of xyloglucan and confirms the drug release-triggering mechanism by the colonic microbiome. Considerable release acceleration by bacterial xyloglucanase was demonstrated with these tablets *in vitro* [16]. Caffeine release rates of 65 and 105 μmol/h were measured at 0.1 and 1 U/mL xyloglucanase concentration, respectively. The deduced *in vivo* value for large intestine of $k_{rel,li}$ = 30.9 μmol/h in the present work is broadly comparable with the *in vitro* results considering the differences in media volume, texture and composition [63,64]. Notably, the xyloglucanase activity concentration determined in rectal and cecal samples (Fig. 10) is within the range of the *in vitro* values corroborating these release rates. This work, hence, demonstrates an interesting example of *in vitro – in vivo* correlation in colonic drug delivery.

The absolute systemic bioavailability of caffeine of 77.4% after IR administration was in line with reported data for oral caffeine dosing in pig [57] and man [50]. A still reduced bioavailability was observed for the CCR caffeine tablets yielding considerably slow controlled drug release yet no evidence of pre-systemic caffeine metabolism that might contribute to this effect can be found in the literature. It can be ruled out, however, that this reduced bioavailability is due to poor absorption or incomplete release of the drug from the tablets since only a very limited caffeine amount was recovered in the fecal droppings (Fig. 9). Pharmacokinetic analysis revealed that constant caffeine release continued for and was completed within 19.9 h after large intestinal arrival. This duration is within the colonic transit time of the animals (Table 2) and is compatible with typical colonic transit time in man [65] underlining the capacity of these CCR tablets for efficient colonic delivery.

The obtained 67.0% absolute systemic bioavailability after IR 5-ASA administration was despite the inclusion of the main metabolite lower than in previous reports describing rapid 5-ASA absorption from the upper gastrointestinal tract in man [44]. The comparatively low dose in combination with slow dissolution and extensive pre-systemic metabolism (see discussion above) are likely responsible for this result. The still lower bioavailability of CCR 5-ASA tablets, providing controlled slow release, is probably related to the non-linearity of the pre-systemic intestinal metabolism and/or the reported diminished efficiency of absorption from distal regions of the gastrointestinal tract [44,52]. The substantial amount of Ac-5-ASA metabolite recovered in the fecal droppings for the IR and the CCR form (Fig. 9) indicates intestinal epithelial metabolism and metabolite efflux into the lumen, given that the colonic microbiome has reportedly a negligible acetylation capacity [46,66,67]. The results also demonstrate complete release of 5-ASA from the CCR tablets as no parent drug was recovered in the droppings. Deduced release duration of 5-ASA in the large intestine was 7.7 h, being much shorter in comparison to caffeine. This likewise reflects reduced absorption efficiency in the large intestine and the dominating epithelial pre-systemic metabolism in combination with apical metabolite efflux and is congruent with colonic delivery; this value, nevertheless, likely represents an underestimate of the true release duration from the tablets. Double peaks observed in plasma profiles after CCR 5-ASA administration are hypothesized to correspond to absorption in the small and the large intestine and be due to pH difference between those segments affecting solubility, as well as the onset of enzymatic action in the colon.

Taken together, results of this animal study provide evidence that colonic delivery can be achieved with the developed CCR tablet formulation. While xyloglucanase activity in porcine rectal samples was in line with human data (section 4.4), enzyme concentration is insufficiently characterized in IBD patients. However, considering the broad dietary prevalence of xyloglucan, a complete absence of enzyme activity towards this hemicellulose is seen as unlikely [68]. Yet a fairly large variation of enzymatic activity in man considering also different dietary habits may be expected. Such a variation was actually found in the pigs (Fig. 10) but this was not reflected in the pharmacokinetic data (Table 1). Interestingly and in agreement with this animal study, *in vitro* data demonstrated that a ten-fold difference in enzyme concentration resulted in a less than two-fold difference in drug release rate [16]. This weak dependence of drug release rate on the enzymatic activity is examined in a follow-up mechanistic manuscript which shows that xyloglucan matrix erosion, being largely responsible for drug release, depends primarily on aqueous media ingress velocity into the matrix and xyloglucan dissolution rate and to a lesser degree on enzyme concentration. Therefore, the anticipated enzyme variability in man including that in the state of disease should not be expected to have a jeopardizing influence on colonic delivery performance of the developed CCR dosage form in the clinical setting. Further, a prolonged transit through the proximal large intestine [69,70] as well as transit acceleration in ulcerative colitis patients were reported [71], while free fluid volume may also influence colonic drug delivery. Yet despite the considerable variability of reported colonic transit time in man, release duration of the CCR tablets largely conforms with average transit time values thus assuring local bioavailability of the luminal drug dose at the site of action based in which therapeutic efficacy in man may be expected.

### 4.4. Xyloglucanase activity

Xyloglucanase activity in cecum was lower than in rectal samples for each individual pig, being consistent with an increasing bacterial density from proximal to distal parts of the gastrointestinal tract [72]. Given the median retention time at the ileocecal junction of 43 min [73], CCR matrix degradation by microbial xyloglucanase and concomitant drug release is expected to take place primarily in the colon. No systematic influence of the study protocol – with its recurrent sedation or the employed drug substances – on xyloglucanase activity and thus the microbial digestive capacity towards xyloglucan could be detected within data variability.

Measured enzyme activity was comparable to preliminary data obtained for healthy human volunteers [16]. Microbial species distribution in cecal and rectal pig samples was in accordance with previous studies [74,75]. *Firmicutes* and *Bacteroidetes* phyla were dominant in porcine cecal and rectal samples, these two phyla being also predominant in the human colonic microbiome [76]. A comprehensive report on the porcine microbiome is the subject of an upcoming manuscript.

### 4.5. Telemetry and gastrointestinal transit times

The small intestinal transit times between 2.6 and 4.5 h obtained in this study are highly similar to previously reported human [77] and pig [30] data and are in agreement with results of sulfapyridine appearance in plasma after IR tablet administration. Further, small intestinal transit times as measured by the SmartPill® capsule were reported to be comparable to those of monolithic dosage forms [30], providing the basis for the small intestinal transit time of three hours used in the present pharmacokinetic evaluation.

Colonic transit time between 18.8 and 62.8 h varied within previously reported ranges in pigs [30,34] while the correspondence to man is difficult to establish given the variability of reported data [10,65,78]. Colonic transit times measured by the SmartPill® capsule are reportedly comparable to those of monolithic dosage forms [30], whereas large dosage forms progress faster through the colon than small particles [21,79]. The measured values may therefore be regarded as lower limit when used to predict the behavior of the CCR tablet.

The gastric emptying times ranging from 44 to >136 h measured in this study are in a similar range as the 68–233 and 20–118 h reported previously for fasted and fed Landrace pigs, respectively [30]. Size and density of the SmartPill® [21,80], but also physiological and anatomic characteristics of the pigs such as the motor activity [81,82], the size of the pylorus [30], or the shape of their stomach [30] might explain the rather long and variable gastric retention. All studies describing delayed gastric emptying of solids in pigs employed oblong devices with high density such as the SmartPill® [30], the BRAVO [80], or the Heidelberg pH capsule [81,82]. It was reported that several interdigestive migrating motor complex cycles may be necessary for transferring large telemetric capsules from the stomach to the duodenum of pigs [77,83]. However, non-disintegrating tablets could be emptied from fed stomach into the small intestine in as few as 0.08 to 2.2 h after meal ingestion [83]. Further, comparatively short gastric emptying times in the range of 1.5 to 6 h were obtained from scintigraphy measurements in pigs [34]. The results of the present study concerning $t_{lag}$, $t_{max}$ and their good reproducibility are consistent with moderate gastric emptying times for monolithic dosage forms and subsequent drug release in the colon. They do not generally agree with the large and hugely variable gastric emptying time obtained with telemetric devices, although individual deviations should be carefully examined. Differences in size, shape, and density between the CCR tablets and these devices may be responsible for the observed differences in gastric emptying.

Passage from one gastrointestinal compartment to another characterized by relative pH differences were finally supported by temperature and pressure data: Temperature measurements by telemetric capsules during gastric residence are influenced by the temperature of liquid or food ingested [21], while colonic pressures showed a different baseline than small intestinal regions [30].

## 5. Conclusion

Analysis of pharmacokinetic data of two active ingredients, caffeine and 5-ASA, and a marker compound, sulfapyridine, in plasma and in feces including absolute bioavailability and deconvolution-derived intestinal absorption and drug release figures are consistent with colonic delivery and provide compelling evidence that the developed CCR tablet formulation affords predominant drug release in the colon. This represents *in vivo* proof of principle of the dual release control concept consisting of an enteric coating and a microbially-digested xyloglucan matrix for efficient colonic delivery. The domestic pig model provides data reasonably allowing the conclusion that the concept can be applicable in man.

## CRediT authorship contribution statement

**Viviane Doggwiler:** Formal analysis, Investigation, Methodology, Validation, Visualization, Writing – original draft. **Chasper Puorger:** Investigation, Methodology. **Valeria Paredes:** Investigation, Methodology. **Michael Lanz:** Formal analysis, Resources. **Katja M. Nuss:** Methodology. **Georg Lipps:** Conceptualization, Funding acquisition, Project administration, Supervision. **Georgios Imanidis:** Conceptualization, Funding acquisition, Project administration, Software, Supervision, Writing – review & editing.

## Declaration of Competing Interest

The authors declare no competing interests. This work was supported by BRIDGE project nr. 20B2-1_180977 of the Swiss National Science Foundation and Innosuisse.

## Data availability

Data will be made available on request.

## Acknowledgments

The authors thank Dr. Christina Wiezorek, Isabel Heel, and the team of the Vetsuisse faculty of the University of Zurich for animal handling and supervision. The work of Dr. Peter Kronen, and Dr. Dagmar Verdino for study preparation and pig surgery is gratefully acknowledged. The authors thank Jasmin Föhr and Dr. Magdalena Albelda for xyloglucanase activity measurement and bacterial composition analysis, respectively. Critical review of the manuscript by Prof. Theodor Guentert was greatly appreciated.

## Appendix A. Supplementary data

Supplementary data to this article can be found online at https://doi.org/10.1016/j.jconrel.2023.04.047.

## References

[1] C.W. Ko, et al., AGA Clinical practice guidelines on the management of mild-to-moderate ulcerative colitis, Gastroenterology 156 (3) (2019) 748–764.
[2] A. Awad, et al., Clinical translation of advanced colonic drug delivery technologies, Adv. Drug Deliv. Rev. 181 (2022), 114076.
[3] A. Yu, et al., Measurement of in vivo gastrointestinal release and dissolution of three locally acting mesalamine formulations in regions of the human gastrointestinal tract, Mol. Pharm. 14 (2) (2017) 345–358.
[4] A.W. Basit, Advances in colonic drug delivery, Drugs 65 (14) (2005) 1991–2007.
[5] F. Varum, G. Hatton, A. Freire, A. Basit, A novel coating concept for ileo-colonic drug targeting: Proof of concept in humans using scintigraphy, Eur. J. Pharm. Biopharm. 84 (3) (2013) 573–577.
[6] F. Varum, A.C. Freire, R. Bravo, A.W. Basit, OPTICORETM, an innovative and accurate colonic targeting technology, Int. J. Pharm. 583 (2020), 119372.

[7] F. Varum, A.C. Freire, H.M. Fadda, R. Bravo, A.W. Basit, A dual pH and microbiota-triggered coating (PhloralTM) for fail-safe colonic drug release, Int. J. Pharm. 583 (2020), 119379.
[8] A. Foppoli, et al., In vitro and human pharmacoscintigraphic evaluation of an oral 5-ASA delivery system for colonic release, Int. J. Pharm. 572 (2019), 118723.
[9] F. Varum, et al., Targeted colonic release formulations of mesalazine – A clinical pharmaco-scintigraphic proof-of-concept study in healthy subjects and patients with mildly active ulcerative colitis, Int. J. Pharm. 625 (2022), 122055.
[10] M. Koziolek, et al., Intragastric pH and pressure profiles after intake of the high-caloric, high-fat meal as used for food effect studies, J. Control. Release 220 (2015) 71–78.
[11] C. Bott, et al., In vivo evaluation of a novel pH- and time-based multiunit colonic drug delivery system, Aliment. Pharmacol. Ther. 20 (3) (2004) 347–353.
[12] M.A. Peppercorn, P. Goldman, The role of intestinal bacteria in the metabolism of salicylazosulfapyridine, J. Pharmacol. Exp. Ther. 181 (3) (1972) 555–562.
[13] D.A. Adkin, et al., The use of scintigraphy to provide 'proof of concept' for novel polysaccharide preparations designed for colonic drug delivery, Pharm. Res. 14 (1) (1997) 103–107.
[14] F. Tuğcu-Demiröz, F. Acartürk, S. Takka, Ö. Konuş-Boyunağa, In-vitro and in-vivo evaluation of mesalazine–guar gum matrix tablets for colonic drug delivery, J. Drug Target. 12 (2) (2004) 105–112.
[15] L. Yang, et al., Effect of colonic lactulose availability on the timing of drug release onset in vivo from a unique colon-specific drug delivery system (CODESTM), Pharm. Res. 20 (3) (2003) 429–434.
[16] V. Doggwiler, M. Lanz, V. Paredes, G. Lipps, G. Imanidis, Tablet formulation with dual control concept for efficient colonic drug delivery, Int. J. Pharm. 631 (2023), 122499.
[17] K. Nishinari, M. Takemasa, J.H.Z. Osaka, R. Takahashi, Storage plant polysaccharides: xyloglucans, galactomannans, glucomannans, in: Comprehensive Glycoscience, Elsevier, 2007, pp. 613–652.
[18] C. Markopoulos, C.J. Andreas, M. Vertzoni, J. Dressman, C. Reppas, In-vitro simulation of luminal conditions for evaluation of performance of oral drug products: choosing the appropriate test media, Eur. J. Pharm. Biopharm. 93 (2015) 173–182.
[19] K. Keohane, M. Rosa, I.S. Coulter, B.T. Griffin, Enhanced colonic delivery of ciclosporin - A self-emulsifying drug delivery system encapsulated in coated minispheres, Drug Dev. Ind. Pharm. 42 (2) (2016) 245–253.
[20] C. Gao, et al., In vitro release and in vivo absorption in beagle dogs of meloxicam from Eudragit® FS 30 D-coated pellets, Int. J. Pharm. 322 (1) (2006) 104–112.
[21] W. Weitschies, L. Müller, M. Grimm, M. Koziolek, Ingestible devices for studying the gastrointestinal physiology and their application in oral biopharmaceutics, Adv. Drug Deliv. Rev. 176 (2021), 113853.
[22] A. Ziegler, L. Gonzalez, A. Blikslager, Large animal models: The key to translational discovery in digestive disease research, Cell. Mol. Gastroenterol. Hepatol. 2 (6) (2016) 716–724.
[23] M. Koziolek, et al., Characterization of the GI transit conditions in beagle dogs with a telemetric motility capsule, Eur. J. Pharm. Biopharm. 136 (2019) 221–230.
[24] R.M. Fancher, H. Zhang, B. Sleczka, G. Derbin, R. Rockar, P. Marathe, Development of a canine model to enable the preclinical assessment of pH-dependent absorption of test compounds, J. Pharm. Sci. 100 (7) (2011) 2979–2988.
[25] J. Kvetina, Z. Svoboda, M. Nobilis, J. Pastera, P. Anzenbacher, Experimental Goettingen minipig and beagle dog as two species used in bioequivalence studies for clinical pharmacology (5-aminosalicylic acid and atenolol as model drugs), Gen. Physiol. Biophys. 18 (1999) 80–85. Spec No.
[26] G. Bode, et al., The utility of the minipig as an animal model in regulatory toxicology, J. Pharmacol. Toxicol. Methods 62 (3) (2010) 196–220.
[27] L.J. Henze, N.J. Koehl, J.P. O'Shea, E.S. Kostewicz, R. Holm, B.T. Griffin, The pig as a preclinical model for predicting oral bioavailability and in vivo performance of pharmaceutical oral dosage forms: a PEARRL review, J. Pharm. Pharmacol. 71 (4) (2019) 581–602.
[28] M.M. Swindle, A. Makin, A.J. Herron, F.J. Clubb, K.S. Frazier, Swine as models in biomedical research and toxicology testing, Vet. Pathol. 49 (2) (2011) 344–356.
[29] L.J. Henze, N.J. Koehl, J.P. O'Shea, R. Holm, M. Vertzoni, B.T. Griffin, Toward the establishment of a standardized pre-clinical porcine model to predict food effects – Case studies on fenofibrate and paracetamol, Int. J. Pharm. X 1 (2019), 100017.
[30] L.J. Henze, et al., Characterization of gastrointestinal transit and luminal conditions in pigs using a telemetric motility capsule, Eur. J. Pharm. Sci. 156 (1) (2020) 105627.
[31] A.M. Rowan, P.J. Moughan, M.N. Wilson, K. Maher, C. Tasman-Jones, Comparison of the ileal and faecal digestibility of dietary amino acids in adult humans and evaluation of the pig as a model animal for digestion studies in man, Br. J. Nutr. 71 (1) (1994) 29–42.
[32] F.N. Hussain, R.A. Ajjan, S.A. Riley, Dose loading with delayed-release mesalazine: a study of tissue drug concentrations and standard pharmacokinetic parameters, Br. J. Clin. Pharmacol. 49 (4) (2000) 323–330.
[33] C. Suenderhauf, G. Tuffin, H. Lorentsen, H.-P. Grimm, C. Flament, N. Parrott, Pharmacokinetics of paracetamol in Göttingen minipigs: In vivo studies and modeling to elucidate physiological determinants of absorption, Pharm. Res. 31 (10) (2014) 2696–2707.
[34] S.S. Davis, L. Illum, M. Hinchcliffe, Gastrointestinal transit of dosage forms in the pig, J. Pharm. Pharmacol. 53 (1) (2001) 33–39.
[35] P.R. Hilfiker, et al., Comparison of three dimensional magnetic resonance imaging in conjunction with a blood pool contrast agent and nuclear scintigraphy for the detection of experimentally induced gastrointestinal bleeding, Gut 45 (4) (1999), pp. 581 LP – 587.
[36] A. Sinha, D.J. Ball, A.L. Connor, J. Nightingale, I.R. Wilding, Intestinal performance of two mesalamine formulations in patients with active ulcerative colitis as assessed by gamma scintigraphy, Pr. gastroenterol 27 (10) (2003) 56–69.
[37] M. Katsuma, et al., Scintigraphic evaluation of a novel colon-targeted delivery system (CODESTM) in healthy volunteers, J. Pharm. Sci. 93 (5) (2004) 1287–1299.
[38] H. Wray, R. Joseph, M. Palmen, D. Pierce, A pharmacokinetic and scintigraphic comparison of MMXTM mesalamine and delayed-release mesalamine: 1110, Off. J. Am. Coll. Gastroenterol. | ACG 103 (2008).
[39] H. Tozaki, et al., Validation of a pharmacokinetic model of colon-specific drug delivery and the therapeutic effects of chitosan capsules containing 5-aminosalicylic acid on 2,4,6-trinitrobenzenesulphonic acid-induced colitis in rats, J. Pharm. Pharmacol. 51 (10) (1999) 1107–1112.
[40] A.K. Azad Khan, S.C. Truelove, J.K. Aronson, The disposition and metabolism of sulphasalazine (salicylazosulphapyridine) in man, Br. J. Clin. Pharmacol. 13 (4) (1982) 523–528.
[41] S. Klein, M.W. Rudolph, B. Skalsky, H.-U. Petereit, J.B. Dressman, Use of the BioDis to generate a physiologically relevant IVIVC, J. Control. Release 130 (3) (2008) 216–219.
[42] S.A. Peters, Physiologically based pharmacokinetic (PBPK) modeling and simulations: principles, methods, and applications in the pharmaceutical industry, 2nd ed., John Wiley & Sons, 2021.
[43] Klaus Schittkowski, Numerical data fitting in dynamical systems - A practical introduction with applications and software, 1st ed., Springer New York, New York, NY, 2002.
[44] B. Myers, et al., Metabolism and urinary excretion of 5-amino salicylic acid in healthy volunteers when given intravenously or released for absorption at different sites in the gastrointestinal tract, Gut 28 (2) (1987), pp. 196 LP – 200.
[45] S. Bondesen, J. Hegnhøj, F. Larsen, S.H. Hansen, C.P. Hansen, S.N. Rasmussen, Pharmacokinetics of 5-aminosalicylic acid in man following administration of intravenous bolus and per os slow-release formulation, Dig. Dis. Sci. 36 (12) (1991) 1735–1740.
[46] U. Knoll, P. Strauhs, G. Schusser, F.R. Ungemach, Study of the plasma pharmacokinetics and faecal excretion of the prodrug olsalazine and its metabolites after oral administration to horses, J. Vet. Pharmacol. Ther. 25 (2) (2002) 135–143.
[47] C. Markopoulos, M. Vertzoni, M. Symillides, F. Kesisoglou, C. Reppas, Two-stage single-compartment models to evaluate dissolution in the lower intestine, J. Pharm. Sci. 104 (9) (2015) 2986–2997.
[48] M.A.B. da Costa, A.L.V. Villa, S.A. Barros, E. Ricci-Júnior, E.P. Dos Santos, Development, characterization and evaluation of the dissolution profile of sulfasalazine suspensions, Brazilian J. Pharm. Sci. 51 (2015) 449–459.
[49] S.H. Yalkowsky, Y. He, P. Jain, Handbook of aqueous solubility data, 2nd ed., CRC Press, Boca Raton, 2010.
[50] G.H. Kamimori, et al., The rate of absorption and relative bioavailability of caffeine administered in chewing gum versus capsules to normal healthy volunteers, Int. J. Pharm. 234 (1) (2002) 159–167.
[51] L.J. Henze, B.T. Griffin, M. Christiansen, C. Bundgaard, P. Langguth, R. Holm, Exploring gastric emptying rate in minipigs: Effect of food type and pre-dosing of metoclopramide, Eur. J. Pharm. Sci. 118 (2018) 183–190.
[52] S.Y. Zhou, D. Fleisher, L.H. Pao, C. Li, B. Winward, E.M. Zimmermann, Intestinal metabolism and transport of 5-aminosalicylate, Drug Metab. Dispos. 27 (4) (1999) 479–485.
[53] F. Karkossa, S. Klein, A biopredictive in vitro comparison of oral locally acting mesalazine formulations by a novel dissolution model for assessing intraluminal drug release in individual subjects, J. Pharm. Sci. 107 (6) (2018) 1680–1689.
[54] D.L. French, J.W. Mauger, Evaluation of the physicochemical properties and dissolution characteristics of mesalamine: relevance to controlled intestinal drug delivery, Pharm. Res. 10 (9) (1993) 1285–1290.
[55] A. Menozzi, C. Mazzoni, P. Serventi, P. Zanardelli, S. Bertini, Pharmacokinetics of oral caffeine in sows: a pilot study, Large Anim. Rev. 21 (5) (2015) 207–210.
[56] M. Bonati, R. Latini, G. Tognoni, J.F. Young, S. Garattini, Interspecies comparison of in vivo caffeine pharmacokinetics in man, monkey, rabbit, rat and mouse, Drug Metab. Rev. 15 (7) (1984) 1355–1383.
[57] M. Mogi, et al., Simultaneous pharmacokinetics assessment of caffeine, warfarin, omeprazole, metoprolol, and midazolam intravenously or orally administered to microminipigs, J. Toxicol. Sci. 37 (6) (2012) 1157–1164.
[58] F. Magkos, S.A. Kavouras, Caffeine use in sports, pharmacokinetics in man, and cellular mechanisms of action, Crit. Rev. Food Sci. Nutr. 45 (7–8) (2005) 535–562.
[59] B.B. Fredholm, Methylxanthines, Springer, Berlin Heidelberg, 2010.
[60] R. Newton, L.J. Broughton, M.J. Lind, P.J. Morrison, H.J. Rogers, I.D. Bradbrook, Plasma and salivary pharmacokinetics of caffeine in man, Eur. J. Clin. Pharmacol. 21 (1) (1981) 45–52.
[61] S. Bondesen, et al., Steady-state kinetics of 5-aminosalicylic acid and sulfapyridine during sulfasalazine prophylaxis in ulcerative colitis, Scand. J. Gastroenterol. 21 (6) (1986) 693–700.
[62] U. Klotz, Clinical pharmacokinetics of sulphasalazine, its metabolites and other prodrugs of 5-aminosalicylic acid, Clin. Pharmacokinet. 10 (4) (1985) 285–302.
[63] K. Murray, et al., Magnetic resonance imaging quantification of fasted state colonic liquid pockets in healthy humans, Mol. Pharm. 14 (8) (2017) 2629–2638.
[64] M. Vertzoni, et al., Biorelevant media to simulate fluids in the ascending colon of humans and their usefulness in predicting intracolonic drug solubility, Pharm. Res. 27 (10) (2010) 2187–2196.
[65] A.Y. Abuhelwa, D.J.R. Foster, R.N. Upton, A quantitative review and meta-models of the variability and factors affecting oral drug absorption - part II: Gastrointestinal transit time, AAPS J. 18 (5) (2016) 1322–1333.

[66] A. Ireland, J.D. Priddle, D.P. Jewell, Acetylation of 5-aminosalicylic acid by isolated human colonic epithelial cells, Clin. Sci. 78 (1) (1990) 105–111.
[67] H. Allgayer, et al., Colonic N-acetylation of 5-aminosalicylic acid in inflammatory bowel disease, Gastroenterology 97 (1) (1989) 38–41.
[68] J. Larsbrink, et al., A discrete genetic locus confers xyloglucan metabolism in select human gut Bacteroidetes, Nature 506 (7489) (2014) 498–502.
[69] A.M. Haase, et al., Regional gastrointestinal transit times in severe ulcerative colitis, Neurogastroenterol. Motil. 28 (2) (2016) 217–224.
[70] S.G. Nugent, D. Kumar, E.T. Yazaki, D.F. Evans, D.S. Rampton, Gut pH and transit time in ulcerative colitis appear sufficient for complete dissolution of pH-dependent 5-ASA-containing capsules, Gastroenterology 118 (4) (2000) A781. Part 1.
[71] J. Fallingborg, L.A. Christensen, B.A. Jacobsen, S.N. Rasmussen, Very low intraluminal colonic pH in patients with active ulcerative colitis, Dig. Dis. Sci. 38 (11) (1993) 1989–1993.
[72] E.T. Hillman, H. Lu, T. Yao, C.H. Nakatsu, Microbial ecology along the gastrointestinal tract, Microbes Environ. 32 (4) (2017) 300–313.
[73] M. Pišlar, H. Brelih, A. Mrhar, M. Bogataj, Analysis of small intestinal transit and colon arrival times of non-disintegrating tablets administered in the fasted state, Eur. J. Pharm. Sci. 75 (2015) 131–141.
[74] D. Crespo-Piazuelo, et al., Characterization of bacterial microbiota compositions along the intestinal tract in pigs and their interactions and functions, Sci. Rep. 8 (1) (2018) 12727.
[75] M. He, et al., Evaluating the contribution of gut microbiota to the variation of porcine fatness with the cecum and fecal samples, Front. Microbiol. 7 (2016).
[76] E.C. Rose, A.T. Blikslager, A.L. Ziegler, Porcine models of the intestinal microbiota: The translational key to understanding how gut commensals contribute to gastrointestinal disease, Front. Vet. Sci. 9 (2022).
[77] M. Koziolek, et al., Investigation of pH and temperature profiles in the GI tract of fasted human subjects using the Intellicap® system, J. Pharm. Sci. 104 (9) (2015) 2855–2863.
[78] F. Schneider, et al., Resolving the physiological conditions in bioavailability and bioequivalence studies: Comparison of fasted and fed state, Eur. J. Pharm. Biopharm. 108 (2016) 214–219.
[79] C.G. Wilson, The transit of dosage forms through the colon, Int. J. Pharm. 395 (1) (2010) 17–25.
[80] C. Suenderhauf, N. Parrott, A physiologically based pharmacokinetic model of the minipig: Data compilation and model implementation, Pharm. Res. 30 (1) (2013) 1–15.
[81] M. Hossain, W. Abramowitz, B.J. Watrous, G.J. Szpunar, J.W. Ayres, Gastrointestinal transit of nondisintegrating, noneridible oral dosage forms in pigs, Pharm. Res. 7 (11) (1990) 1163–1166.
[82] R.L. Oberle, H. Das, Variability in gastric pH and delayed gastric emptying in yucatan miniature pigs, Basic Pharm. Res. 11 (1994) 592–594.
[83] A.J. Coupe, S.S. Davis, D.F. Evans, I.R. Wilding, Correlation of the gastric emptying of nondisintegrating tablets with gastrointestinal motility, Pharm. Res. 8 (10) (1991) 1281–1285.